university of groningen / faculty of science and engineering

Catalytic hydrotreatment of Kraft lignin: oil yield improvements by pretreatment of lignin using ball milling

Master research project

August 24, 2021

Student: J.R.J. Strien (s2943263)

Primary supervisor: prof. dr. ir. H.J. Heeres

Secondary supervisor: dr. P.J. Deuss

Daily Supervisor: H. Yang

Abstract

Lignin is the most widely available renewable source of aromatics, and it has gained increased attention from scientists around the world to utilize these aromatics for renewable chemicals. In this study, the effect of mechanical pretreatment of Kraft lignin with solvent-free catalytic hydrotreatment is examined. A phosphide NiMo catalyst was used in a batch autoclave reactor at a temperature of 400 °C for 2 hours with an initial pressure of 100 bar H_2 to hydrotreat the lignin. The catalyst was characterized by BET, XRD, and NH_3-TPD, the lignin and the ball milling process were characterized by HSQC, NMR and XRF, and the reaction products were characterized with Karl-Fisher titration, TGA, EA, ICP, GPC, GCxGC. Ball milling lignin prior to solvent-free catalytic hydrotreatment resulted in a 35% reduction in solids produced and an increase of 13% on oil yield. Monomeric yield remained the same relative to the oil yield.

Contents

ACKNOWLEDGEMENTS

This work would not be possible without the continued insight and help provided by H. Yang for the whole duration of the project. Additionally, I would like to express gratitude to the analysis department, in specific L. Rohrbach and G.J. Boer, for the help, training and patience with analysis. Lastly, I would like to thank the Chemical Engineering department, in particular H.J. Heeres and P.J. Deuss for their ideas and insight.

Chapter 1

INTRODUCTION

Biomass is organic matter that is readily renewable. Commonly, biomass is associated with plant life, such as trees, agricultural crops and wastes and energy crops. In the short list of renewable resources (including solar energy, wind energy), biomass is the only means of renewable carbon in nature. With an ever increasing demand for energy, and countries investing in increasing the share of renewables in their energy production, the demand for renewable resources is increasing.

The most abundant form of biomass is lignocellulosic biomass. Lignocellulosic biomass' main components are cellulose, hemicellulose and lignin. Cellulose is a biopolymer from glucose units and hemicellulose is a biopolymer of C5 and C6 sugars, such as xylose, arabinose, mannose, and galactose [1]. Lignin is a complex 3D branched polymer of aromatic subunits. Examples of lignocellulosic biomass are wood pulp, corn stovers and many agricultural waste products. The application of lignocellulosic biomass is well established in biofuels and specialty chemical production, such as bioethanol fermentation from cellulose or enzymatic transformation to a wide range of chemicals.

Currently, only 2% of the globally produced lignin is used in specialty chemicals [2], and the remaining 98% is used for heating value. In the past decades, innovations in valorization have allowed for a more efficient transformation of the lignin into higher value chemicals. With an increasing amount of publications in the field of lignin valorization [3], the scientific community shows increasing interest in the practical applications of renewable aromatics.

The utilization of lignin of the lignocellulosic biomass is considered a major part of future biorefineries for renewable resources because as described by four major points by Li et al. [4]. (1) Effective valorization and utilization of lignin, which accounts for 10-35% of the biomass, will make a larger portion of the feedstock economically viable in contrast to the current heating value. (2) The aromatic subunits of lignin are by far the most common re-

newable source of aromatic units in nature, which makes lignin a contender for the feedstock of aromatic monomers, a market which is dominated by fossil resources [5]. (3) Lignin protects the cellulose and hemicellulose from chemical and biological modifications [6]. Effective valorization will allow for more accessible use of cellulose and hemicellulose. Lastly (4) the paper pulp industry produces 7 tonnes of black liquor per tonne of paper pulp [7]. Black liquor is a waste stream rich in lignin. Utilization of this lignin waste stream will have positive environmental effects.

1.1 Lignin

This section will primarily describe the lignin on a molecular level, common functional groups that can be found in different lignin types and the isolation of different lignin types and their differences.

1.1.1 Building blocks

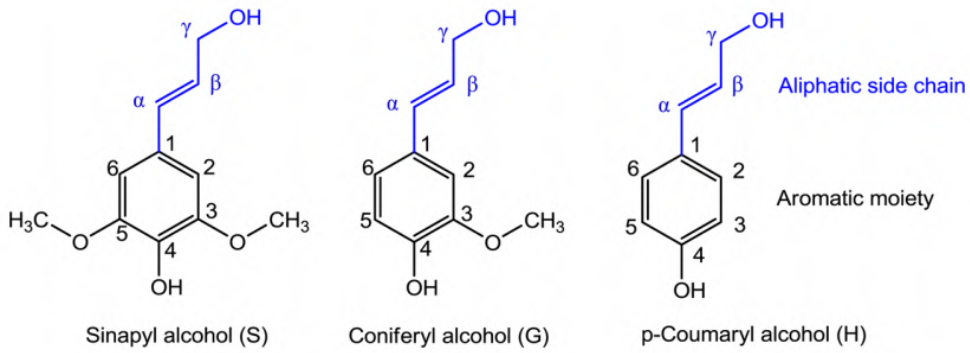

Figure 1.1: Main monomers for lignin [4]

On a molecular level, lignin is a branched, three-dimensional polymer mainly consisting of three main monomers (see Figure 1.1):

1. Sinapyl alcohol. Also known as syringyl, or S unit. 3,5-dimethoxy-4-hydroxycinnamyl,

2. Coniferyl alchohol. Also known as guaicyl, or G unit. 3-methoxy-4-hydroxycinnamyl and

3. *p*-coumaryl alcohols. Also known as p-hydroxyphenyl, or H unit. 4-hydroxycinnamyl

These monomers are linked with ether and C-C bonds. The common factor in these monomers is their phenolic central group with a C3 unsaturated alcohol side chain. The central group is generally referred to as a phenylpropane unit (ppu). The differentiating factor between these monomers is the number of methoxy functional groups on adjacent carbons regarding the phenlolic alcohol.

The carbons on the aliphatic side chain are denoted with α, β and γ, with α being the carbon directly bound to the aromatic ring and γ being the terminal carbon attached to the hydroxyl. For the aromatic unit, the carbons are numbered as such the aliphatic side chain starts at 1, and then according to standard UIPAC rules, increasing in a circular direction where a methoxy side chain is either at position 3 in the case of a single methoxy, or at positions 3 and 5 for a dimethoxy. The hydroxyl is always located at position 4. These denotations are relevant for the description of the phenylpropane unit linkages.

Different types of biomass (hardwoods, softwoods and grasses), have different compositions of the S, G and H units: grasses tend to have a mixture of all three, while softwoods generally contain mostly G-units. Hardwoods consist of mainly S-units, followed by G-units and only trace amount of H-units [8].

In addition to these three main monomers, different types of biomass incorporate different chemical species in the polymer network, including ferulic acid, ferulates and more [9, 10].

1.1.2 Linkages and functional groups

Lignin monomers are mainly linked with ether and carbon carbon bonds. To distinguish, the linkages are named based on their carbon location and the type of bond, as shown in Figure 1.2.

The proportion of each linkage varies by type of biomass. For soft and hardwoods, these proportions are shown in table 1.1. For modified lignins, such as Kraft, Lignoboost and Organosolv, these linkages can be quite different.

Linkages are either ethers or carbon-carbon bonds. Ethers are described $x-O-y$ links and carbon-carbon bonds are shown as $x-y$ linkages, where x and y denote carbons on either the aliphatic side chain (greek letters) or the aromatic unit (numbers).

Figure 1.3 shows a model of lignin with identified monomer structures and linkage types

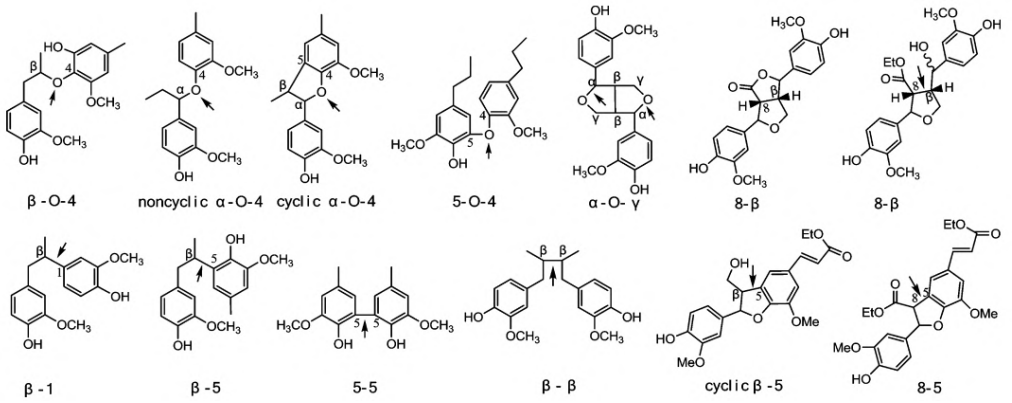

Figure 1.2: Linkage types [4]

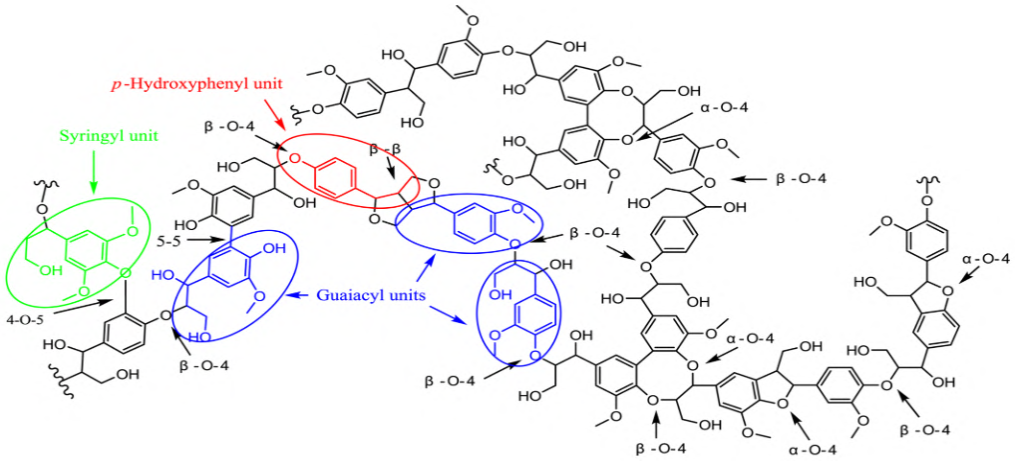

Figure 1.3: Representative structure model of lignin with identified monomer structures and linkage types [4]

1.1.3 Isolation of technical lignin

Lignocellulosic biomass in itself is not edible for humans. Therefore the usage of lignocellulosic biomass as a renewable resource does not negatively impact food supply. In addition to its abundance, it is therefore widely considered as a promising alternative for fossil-based fuels and chemicals. In order to use the lignin as a feedstock for value-added processes, it needs to be isolated first.

Lignin is a complicated structure and the extraction of lignin is not straight forward as it is bound to the cellulose and the hemicellulose. Additionally, the lignin differs from feedstock to feedstock. The main hurdle is to produce pure lignin without compromising on the structure or isolation

Table 1.1: Lignin linkage and functional group proportion in soft and hardwoods. Number per 100 ppu (phenylpropane unit) [11, 12].

	Number/100 ppu			Number/100 ppu	
Linkage	Softwood	Hardwood	Functional group	Softwood	Hardwood
β-O-4	43-50	50-65	Methoxyl	92-96	132-146
β-5	9-12	4-6	Phenolic hydroxyl	20-28	9-20
α-O-4	6-8	4-8	Benzyl hydroxyl	16	
β-β	2-4	3-7	Aliphatic hydroxyl	120	
5-5	10-25	4-10	Carbonyl	20	3-17
4-O-5	4	6-7	Carboxyl		11-13
β-1	3-7	5-7			
Others	16	7-8			

yield. For lignin to be extracted, it needs to be depolymerized from the hemicellulose and cellulose [13]. Most common methods include extraction, sulfur addition and base or acid catalyzed depolymerization [4, 14].

It has been shown that lignin composition and contents vary per type of biomass. For example, in softwoods, the lignin composition is approximately 30% by weight, while for hardwoods this is in the range of 20-25 % by weight. In grassy biomass, lignin composition is only around 10-15 % of the total weight [4]. Also, the composition of the lignin across different types of biomass can vary greatly.

Milled Wood Lignin (MWL) and Cellulolytic enzyme Lignin (CEL)

The use of ball milling for applications regarding lignin extraction goes back several decades. In 1957, it was reported by Björkman that milling the wood and subsequently extracting the lignin could return yields of up to 50 % while the molecular composition of lignin was altered compared to native lignin (Browns Native Lignin, BNL) [14, 16]. MWL contained less phenolic hydroxyl functionality, in line with other methods of extracting lignin such as lignosulfonate.

CEL and MWL are very similar methods for extracting lignin from wood, as they use a similar pathway with milling and extraction, see Figure 1.4. Only after the second extraction step, with 96% dioxane, the MWL and

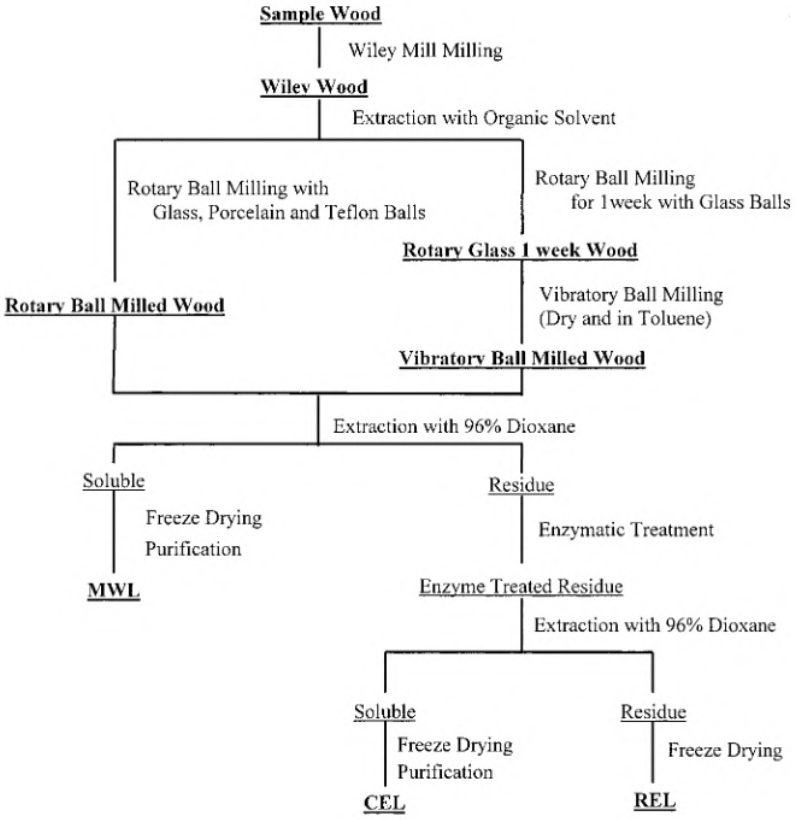

Figure 1.4: MWL and CEL extraction pathway [15]

CEL are extracted from the two different fractions of this step. Therefore it is logical that the molecular structure of CEL and MWL are similar, as the remaining steps are relatively mild.

Chang et al. examined the structure of milled wood lignin (MWL). They showed that milled wood lignin has increased carbonyl content and phenolic hydroxyl groups while observing decreased molecular weight [17]. Despite these differences, they concluded that the MWL is an adequate representation of lignin in wood, but cellulolytic enzyme lignin (CEL) was obtainable with better yields and with less degradation. This was later debated by Whiting and Goring as they showed that MWL was not representative for the total lignin in wood, but rather only of the secondary cell wall [18].

In 2002, Ikeda et al. published a paper that examined the differences between MWL and CEL using a derivatization followed by reductive cleavage (DFRC) method and they corroborated the findings of Chang et al [15]. In addition, they found the structure of the MWL to be identical to CEL, with the small changes in functional groups. In general, MWL is accepted to

represent the native lignin structure, but at a note that β-aryl ethers can be cleaved into hydroxyl groups during the ball milling process. Moreover, this can increase the amount of α-carbonyl groups as a result of side-chain oxidation.

Kraft

Kraft lignin is a sulphur-containing, heavily chemically modified type of lignin that is produced as a byproduct of the Kraft process, which accounts for 85% of the total lignin production in the world as of 2015 [19]. The Kraft process converts wood into pulp by cooking wood chips in a solution of sodium hydroxide and sodium sulfide [2] at 150-170 °C [20] with fairly high yield: about 90 % of the lignin is extracted by the sodium-containing solution. During the process, specific β-O-4 bonds are broken promoted by alkali induced deprotonation [21], causing the molecular weight of the material to decrease. Also, the molecular structure of the lignin is heavily modified due to the incorporation of sulfur. These fractured lignin molecules create a dark brown solution. After separating the lignin from the solution, a brown powder is obtained. The main application of Kraft lignin is heat recovery in industrial processes, as there has not been an effective industrial process for higher value applications as of yet.

Lignosulfonate

Similar to Kraft lignin, the lignosulfonate process also utilizes sulfur and pulping to separate lignin from the (hemi-)cellulosic biomass. The main difference is in the chemicals used for this process as the lignosulfonate process utilizes sodium bisulfite and sodium sulfite [19]. During the pulping process, certain functional groups of side chains of the aromatic compounds, the phenyl propanes, are attacked by bisulfite ions in the presence of acid (see Figure 1.1). These groups allow for the lignin to be dissolved in water. Most of the cellulose is untouched by this process, however a small amount is modified to form water-soluble monosaccharides. Lignosulfonate is widely used for industrial lignin utilization due to its sulfonic side groups and solubility in water as binder, dispersant, retarder or emulsifier.

Soda Lignin

The soda-anthraquinone pulping process uses sodium hydroxide as the main chemical to pulp the lignin without the incorporation of sulfur. The soda pulping process applies to annual plants [22], like grasses, straw and flax, which cause the black liquor from this pulping process to have high ash

(silicon) contents. Using acid precipitation and washing, high purity lignin can be obtained.

Instead of sodium hydroxide, lithium hydroxide or potassium hydroxide has also been used. The hydroxide cleaves the β-O-4 bond in the lignin, which is the weakest bond in the lignin, in order to depolyermerize the lignin [23].

Organosolv

Organolsolv lignin is produced by dissolving the lignin in organic solvents at at high pressure and elevated temperature, which break specific aryl ether bonds (α-O-4) [24] in the lignin causing it to dissolve in the medium. Using the solubility of the lignin in organic compounds and subsequently precipitating using water yields high purity lignin [19]. Yields can be higher than in the Kraft extraction process. The organic solvent can be recycled through the process [25]. Organosolv extraction is generally milder than other types of extraction [26], as alcohol integration can protect the polymer structure whereas fractionation in other methods are performed at higher temperatures.

Typical solvents for this process are a mixture of water and an organic solvent such as ethanol or methanol, but ethanol is preferred due to its low cost and easy recovery [25]. Fractionation using formic acid has shown to improve the extraction of lignin and solvents like acetone have also shown use-cases [27].

A specific type of Organosolv extraction is the Alcell Process using a 60/40 mixture of ethanol and water [25]. As lignin depolymerizes and creates very small particles, hemicellulose hydrolyses and dissolves, the ethanol content is reduced by destillation and the insoluble cellulose is separated. Water and acids are added to precipitate out the lignin.

Linkages in different technical lignins

Constant and colleagues quantified the chemical nature of Kraft, Soda lignin, organosolv and Alcell lignin with respect to the composition, free hydroxyl groups, typical inter-unit linkages and average molar mass [28].

The researchers compared six types of lignin: (Softwood) Indulin Kraft, (Straw and grass) Soda P1000, (Hardwood) Alcell, Organosolv from Wheat straw (OS-W), poplar (OS-P), which is a hardwood, and spruce (OS-S), a softwood, on aforementioned contents. These results can be seen in Table 1.2 to 1.5. Kraft, Soda and Alcell lignin are readily produced at industrial scale, while OS-W, OS-P, and OS-S much less. The main differences between technical lignins in the described research are summed below.

- Kraft and Soda lignin have a larger portion of soluble components. Additionally, Soda lignin has a large part of acid-soluble lignin. Alcell lignin is a more pure variant of lignin, with a trance amount of ash, which can be attributed to the method of extraction.

- Total phenolic hydroxyl content is highest in the Alcell extraction process (3.3), where the other processes outlined in the research are very similar between 2.5 and 2.9 mmol/g dry lignin.

- Kraft and spruce lignin are very similar in that they contain a large number of G units, whereas the hardwood and grass lignin have S and G units both significantly present. Soda lignin and Wheat organosolv are the only two types with the completely demethoxylated H units.

- Poplar and spruce organosolv lignin have little and no β-O-4 bonds, while wheat organsolv and other technical lignins have significant amounts (3.4-6.1[1] per 100 ppu).

- The number average molecular weight (M_n) of Soda and Alcell lignin are the highest of all examined lignin types. They are slightly higher than the hardwood, poplar organosolv, and Kraft lignin and much higher than the softwood and wheat organosolv. The differences in molecular weight can be directly attributed to the severity of the pulping process [28]. Additionally, the polydispersity of all lignin types is similar (3.8-5.2) except Kraft lignin, which is 8.1.

[1]based on only S and G functionality, as Soda lignin and OS-W have a portion of H units, the actual β-O-4 content is higher

Table 1.2: Technical lignin content based on dry weight. AIL: Acid insoluble lignin, ASL: Acid Soluble lignin. Adapted from Constant [28]

	Lignin		Carbohydrates						Ash	Sum
	AIL	ASL	Arabinan	Xylan	Galactan	Glucan	Mannan	Sum		
Indulin Kraft	90.3	1.9	0.1	0.6	0.6	0.1	<0.1	1.4	2.6	96.2
Soda P1000	85.1	5.4	0.2	1.5	0.2	0.5	<0.1	2.4	2.5	95.5
Alcell	94.3	1.9	<0.1	0.1	<0.1	0.1	<0.1	0.2	<0.1	96.4
OS-W	94.1	0.9	0.1	0.2	<0.1	0.2	<0.1	0.5	<0.1	95.6
OS-P	94.3	1.6	<0.1	0.2	<0.1	0.1	<0.1	0.3	<0.1	96.1
OS-S	95.5	0.8	<0.1	0.2	<0.1	0.3	0.6	1.1	<0.1	97.4

Table 1.3: OH in technical lignin expressed as mmol of functional group per g dry lignin, quantified by ^{31}P-NMR. Adapted from Constant [28]

	Aliphatic OH	5-Substituted OH	Guaiacyl OH	p-Hydroxyphenyl OH	Total PhOH	COOH	Free COOH /tricin
Indulin Kraft	1.79	1.31	1.30	0.16	2.77	0.33	0.05
Soda P1000	1.26	1.73	0.73	0.40	2.86	0.80	0.14
Alcell	1.04	1.68	0.58	0.11	3.30	0.22	0.00
OS-W	1.27	1.24	0.92	0.38	2.54	0.21	0.20
OS-P	0.80	1.83	0.58	0.18	2.59	0.07	0.00
OS-S	1.43	1.21	1.44	0.08	2.73	0.06	0.00

Table 1.4: Quantification of aromatic units and side chains in different types of lignin. [1]: Expressed as a number per 100 aromatic units (S + G). [2]: Molar percentage (S + G + H = 100) see also section 1.1.1. Adapted from Constant [28]

	Indulin Kraft	Soda P1000	Alcell	OS-W	OS-P	OS-S
β-O-4[1]	6.1	3.4	5.3	4.3	0.1	0
β-5[1]	0.3	0	0.8	4.5	1.8	3.3
β–β[1]	1.0	0.7	2.8	0.1	1.1	0.2
Total ether side chains[1]	7.4	4.1	8.9	8.9	3	3.5
Stilbenes (St)[1]	2.3	0	0.4	0.4	0	0.7
p-Coumarate (Pca)[1]	0	3.2	0	2.2	0	0
p-Hydroxy benzoate (Pb)[1]	0	0	0	0	9.4	0
Tricin (T)[1]	0	0	0	3.5	0	0
S[2] (%)	0	50	63	39	53	0
G[2] (%)	97	39	37	58	47	100
H[2] (%)	3	11	0	3	0	0
S/G ratio	0	1.3	1.7	0.7	1.2	0
H/G ratio	0	0.3	0	0.1	0	0

Table 1.5: Molar masses (M_w, M_n) expressed in g/mol and polydispersity (PD). Adapted from Constant [28]

	M_w	M_n	PD
Indulin Kraft	4290	530	8.1
Soda P1000	3270	620	5.2
Alcell	2580	600	4.3
OS-W	1960	450	4.4
OS-P	2180	570	3.8
OS-S	2030	420	4.9

1.2 Lignin Valorization

Valorization of lignin is described as a method to make higher value products out of residues. In this context, this applies to using lignin to produce higher quality chemicals. For this to occur, the large polymer chains that range from 600 to 180 000 Da in the case of black liquor from the Kraft pulping process need to be reduced to smaller molecules [29]. For lignin, these can include platform chemicals such as phenols, hydrocarbons or specialized chemicals such as pyruvate and vanillin [30].

1.2.1 Pyrolysis

Pyrolysis is the process in which a substrate is heated in the absence of oxygen which causes the substrate to decompose. For the application of lignin pyrolysis, this means that lignin is heated to depolymerize the network to obtain smaller products. Generally, this means rapid heating in a range of temperatures between 450 °C and 600 °C. In this way, up to 70 wt% of biomass (on a dry basis) can be converted to a liquid product, which is termed pyrolysis oil or pyrolysis liquid [31].

The mechanism of pyrolysis is not fully understood, but based on NMR results a prediction as to which bonds are cleaved can be done. This is schematically shown in Figure 1.5. A pathway through radicals is currently accepted as a mechanism. The pyrolysis cleaves the weakest bonds primarily, the C-O bonds, at lower temperatures. At higher temperatures, C-C bonds also cleave. Even within the types of C-O bonds, differences in dissociation energy are observed. The C_α-O ($\alpha - O - 4$) bond was deemed the weakest and the C_β-O ($\beta - O - 4$) the second weakest [32].

Pyrolysis is also one of the main methods that has been investigated over the years, and therefore the process is far developed. There are a large number of conditions that have been broadly described in the literature, including temperature, pressure, heating rate, lignin type and catalyst. Compared to other methods of valorization, pyrolysis is very cheap.

Conventional pyrolysis has shown a majority of products formed between 400 and 500 °C, where phenolic yields of over 40 % can be observed. Three general competing reactions from pyrolysis radicals can be observed during pyrolysis, with or without catalyst [34]: 1) repolymerization to form char, 2) stabilization to form alkyl phenol, or 3) dehydration or similar to form aromatic hydrocarbons, see also Figure 1.6. Gasses that are formed during the pyrolysis, which are generally CO, CO_2 and CH_4 are likely the results of cracking of -CHO, -COOH and -CH_3. It is suggested that the second and third method of stabilization and reformation of intermediate radicals is

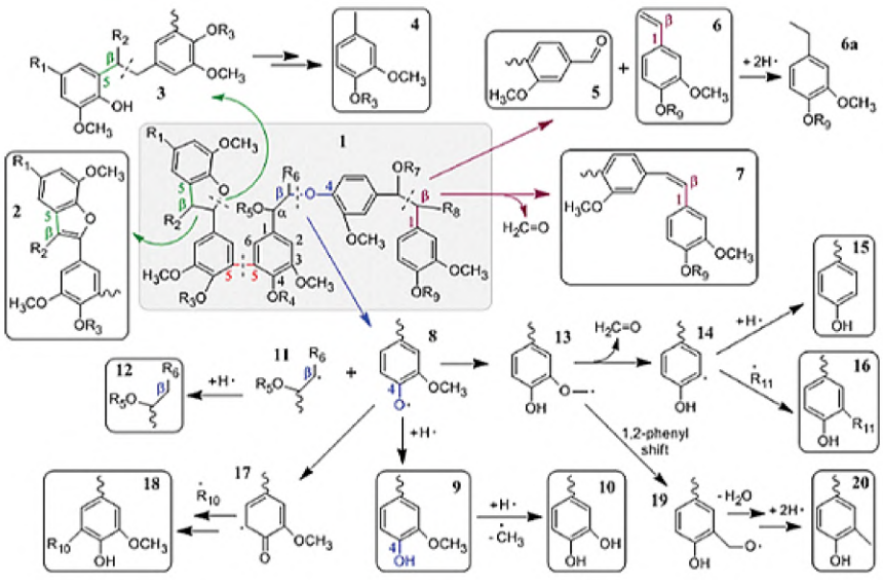

Figure 1.5: Summary of pyrolysis of lignin [4] [33]

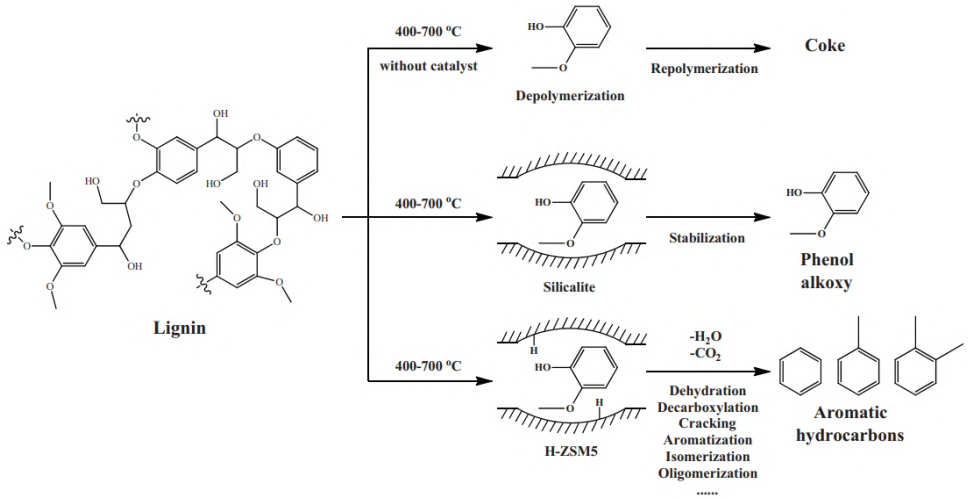

Figure 1.6: Reactions of radical pyrolysis oil intermediates, with acidic sites in a zeolite catalyst [34]

promoted by the acidic sites in the zeolite catalyst. Without the presence of a catalyst, the dominant pathway is the char formation.

1.2.2 Hydroprocessing

Hydroprocessing is the general name for thermal reduction using hydrogen. It has been widely used and is effective and efficient in many types of reactions in depolymerization and reformation.

Hydrogenolysis

Hydrogenolysis is a collective name for the cleavage of a carbon-carbon or carbon-heteroatom using hydrogen [35]. A specific type of hydrogenolysis is the hydrodeoxygenation, or HDO in short. As the name suggests, it removes oxygen from oxygen-containing compounds using hydrogen. HDO is the most relevant type of hydrogenolysis for upgrading bio-oil, as it cleaves the oxygen from the lignin or pyrolysis oil to obtain desired products, like monophenols [36–38] or cycloalkanes [39]. The mechanism for deoxygenation is usually a combination of hydrogenation-deoxygenation or direct deoxygenation [40,41].

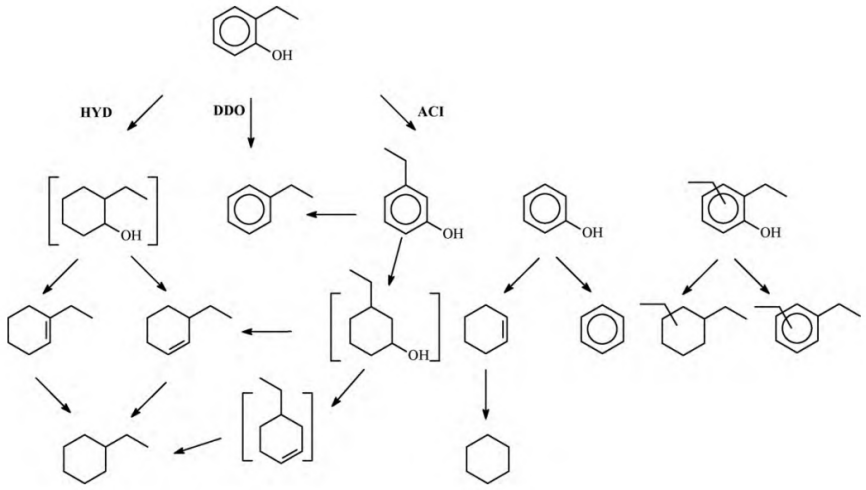

Figure 1.7: Schematic hydrogenolysis of 2-ethylphenol using a MoS catalyt on γ-aluminum oxide [40]. HYD: Hydrogenation, DDO: direct deoxygenation, ACI: side reaction by the acid properties from the catalyst support. Compounds in brackets were not observed in the reaction mixture.

A vast range of catalysts have been tested for this specific purpose, and while many catalysts, e.g. Ru/C and Pd/C, show activity, their activities are attributed to electron configuration of the metal active centre for dissolving molecular H_2 [42]. In general, transition metals on a highly porous support have been shown to work well [4]. Moreover, the addition of a second metal, such as Co or Ni or Mo, to the catalyst has been shown to enhance the

deoxygenation, either through an enhancement of direct deoxygenation or through demethoxylation [40, 43–45].

Apart from single bond cleavage, hydrogen also has the ability to saturate unsaturated bonds in the chemical structure in the presence of catalysts.

1.2.3 Solvent-free Catalytic Hydrotreatment

Solvent-free catalytic hydrotreatment is a type of hydrotreatment where no solvent is used to facilitate good contact between solid lignin and the solid catalyst. This method has been explored in detail the last 2 decades. The process uses lignin with a 5-10 % loading of catalyst and is heated and stirred in a high pressure hydrogen atmosphere to 250-450 °C. The absence of a solvent promises better economic feasibility and a greener process.

Ramesh and colleagues [46] found that catalytic hydrotreatment of lignin over sulfided NiMo and CoMo catalysts without the presence of a solvent is capable of yielding good monomer yields, low solid yields and high conversion in relatively simple chemical circumstances. The support of the catalyst has an effect on its activity and a substantial effect on lignin depolymerization and monomer yield. The sulfided NiMo catalyst on MgO-La_2O_3 yielded the best results with 26.4% monomer yield on lignin intake.

Osorio Velasco and colleagues later found that using a phospided NiMo catalyst on SiO_2 support can even enhance monomer yield to over 50 % [47] and oil yield over 68%, which is the best reported catalyst for Solvent-free HDO so far. The found that an intermediate acidic support such as SiO_2 perfoms best out of a large selection of supports. This support the findings of Ma [34] who suggested that the acidic sites in the catalyst support promote dehydration.

1.2.4 Oxidation

Oxidative cleavage of lignin can break carbon-carbon bonds, ether bonds and even aromatic bonds. The general products are mostly polyfunctional aromatic monomers [4]. Cleavage is commonly done using metal oxide as the catalyst, or strong oxidizing reagents such as molecular oxygen, hydrogen peroxide [48] or nitrobenzene [49]. Drawbacks of this method include extensive re-oligimerization and the low yield on model compounds in order to make this process viable.

1.2.5 Gasification

Gasification of lignin is a method of valorization that produces syngas, a mixture of hydrogen and carbon monoxide. This mixture of gasses can then be upgraded into either liquid fuels with the Fischer-Tropsch synthesis or in a methanol/dimethyl ether synthesis [50–52]. The method of gasification omits the need for drying the biomass with high moisture content, however the process is still very in the developmental stage as it requires many steps, including a gasifier, gas cleanup, water-gas shift and a syngas converter. For each step, the process has to be optimized and catalysts have to be developed, which generates a large problem before this can become a viable process.

1.2.6 Liquid Phase Reforming

In a similar method to Gasification, Liquid Phase reforming (LPR) breaks the material into syngas under milder circumstances than gasification (500K for LPR compared to 773K for gasification) [53]. Common solvents for this process include water, a water/ethanol mixture, supercritical ethanol or ammonia and these have been shown to be able to reform lignin at moderate temperatures and pressures [4]. In specific water, which is the ideal solvent given its low cost and high availability, the lignin needs to undergo cleavage of the abundant β-O-4 linkages and some of the 5-5' linkages prior to LPR. This also found that using LPR followed by HDO yields BTX, which in practice is very similar to the Solvent Free Catalytic Hydrotreatment described above, where some bonds in the lignin are broken using hydrogen and high temperature in liquid phase and subsequent HDO yields BTX.

1.2.7 Base/acid catalyzed depolymerization

Depolymerization of lignin usually uses a strong base or acid as a catalyst. Base-catalyzed depolymerization uses cheap, commercially available bases such as LiOH, NaOH or KOH and predominantly cleaves β-O-4 bonds, which are the weakest bonds [54–56]. As the base catalyzed process takes place at elevated temperatures of 250 to 650 °C, the depolymerization products include char, volatiles and a complex mixture of phenolics and alkylated phenolics.

Acid catalyszed depolymerization follows a similar trend compared to base catalyszed depolymerization as it hydrolyzes aryl ether bonds primarily. The mechanism on the other hand is different, as it is first dehydrated followed by the formation of ketones. The base catalyzed depolymerization cleaves the ether bond more directly.

For both types of depolymerization outlined above, yields and conversions are relatively low in model compounds. Oil yields for direct lignin depolymerization are generally below 50% [4] and significant degradation and char formation can be observed. Additionally, acid-catalyzed depolymerization is rather expensive due to the high cost of the required acids and difficult separation downstream.

1.3 Pretreatment of lignin

Pretreatment for the lignin extraction goes back decades [14] and most research regarding pretreatment focuses on the delignification of biomass [3]. In the extraction of lignin from biomass, the lignin is often already severely modified because of this delignification step. In the case of Kraft lignin, the molecular weight is much lower and there are sulfur containing functional groups introduced compared to lignin in biomass. In this section, the pretreatment of lignin itself (such as Kraft, organosolv etc.) is discussed from an angle of relevance to lignin valorization.

1.3.1 Deep Eutectic Solvent Pretreatment

Pretreatment of technical lignin for downstream applications is less well explored than the pretreatment for the lignin extraction. For a lignin-based phenolic formaldehyde adhesive, the technical Kraft lignin was exposed to a $ZnCl_2$ / lactic acid deep eutectic solvent. Xian and colleagues [57] found that it increased the phenolic hydroxyl content from 3.12 wt% to 3.93 wt% and decreased the methoxy content 11.83 wt% to 6.64 wt% at optimal reaction conditions. The adhesive prepared by this method had improved characteristics over the untreated Kraft lignin.

1.3.2 Mechanochemical Pretreatment

Qu and colleagues have shown that ball milling lignin with ionic liquids is capable of reducing polydispersity, the amount of methoxy groups and the particle size while retaining phenolic hydoxyl groups under certain conditions [58]. In the process of lignin valorization, molecular weight needs to decrease to obtain value-added chemicals.

1.3.3 Mechanical Pretreatment

Kandula and colleagues [59] used ball milling of Kraft lignin as a form of pretreatment for the polyesterification of lignin and ϵ-caprolactone. They used a ball mill at 2000 rpm for 10 minutes and tested different sizes of glass balls for a mixture of ϵ-caprolactone and kraft lignin: 0.8, 1.55 mm, 2 mm, 3 mm and 4 mm. The researchers found that the particle size was reduced in the case with 2 mm balls without any polymerization. Milling with smaller balls lead to the formation of hot-spots, which caused irregular polymerization with ϵ-caprolactone during the milling process and therefore increasing the particle size. The researchers found that the particle size could be reduced from 0.5-70 µm for raw Kraft lignin and ϵ-caprolactone to 0.3-6 µm for the milled mixutre, with the median particle size being reduced from 7.6 to 1.4 µm. The increased surface area from the reduction of particle size lead to improved reaction kinetics with ϵ-caprolacton.

Ikeda et al. [15] have shown that ball milling lignin itself mostly decreases lignin particle size. A denied patent from 2013 (CN103113596A) claimed that dry milling lignin reduces polydispersity and facilitates higher-value transformation of lignin, which has similar effects to the mechanochemical pretreatment in ionic liquids.

1.4 Approach

The main objective of this project is to study the feasibility to improve yields of biobased chemicals from lignin in catalytic hydrotreatment by using mechanical pretreatment.

To achieve this, the project is divided into two main parts. Firstly, the effects of ball milling on the lignin structure will be explored. Secondly solvent-free catalytic hydrotreatment will be used in conjunction with ball milled Kraft lignin and raw Kraft lignin to produce biobased aromatic monomer and other value-added chemicals.

1.5 Relevance

The concept of pretreating biomass to extract lignin is relatively well described. Ball milling and extraction with solvents, acids or bases and sulfonation have been extensively tried and tested. On the other hand, there are many processes of lignin valorization, each with its own advantages and disadvantages. Surprisingly, very little is known about the large-scale pretreatment of industrial lignin, such as Kraft, for valorization. Only a handful

of publications have been found to relate to this subject.

Moreover, the scientific community is seeing the usefulness of lignin as a major renewable source for aromatic compounds [3] and lignin is an essential part of future biorefineries [4]. The combination of applying the pretreatment of lignin with lignin valorization can hopefully give more insight into the practical feasibility of producing aromatic monomers from industrial lignin.

Chapter 2

MATERIALS AND METHODS

2.1 List of Chemicals

Catalyst support silicon dioxide (SiO_2) nanopowder with 95.5% trace metal basis (10-20 nm particle size), nickel(II) nitrate hexahydrate ($Ni(NO_3)_2 \cdot 6H_2O$) $\geq$ 98.5%, ammonium molybdate tetrahydrate ($(NH_4)_6Mo_7O_{24} \cdot 4H_2O$) 99.98 %, 70% nitric acid solution (HNO_3), ammonium phosphate dibasic ($(NH_4)_2HPO_4$) $\geq$ 98% and deuterated dimethyl sulfoxide (d_6 DMSO) 99.5% were obtained from Sigma Aldrich. Analytical grade Acetone, THF and dibutylether were obtained from Boom B.V. Hydrogen ($\gg$ 99.99) was produced by Hoekloos and 1% O_2/N_2 was produced by Linde Gas Benelux B.V.

2.1.1 Lignin feedstock

As a feedstock for the research, Indulin AT Kraft lignin from Ingevity was used. According to the product page, Indulin AT is "a highly purified, unsulfonated raw Kraft lignin. This product is highly functionalized in carboxylic acid, aliphatic and aromatic hydroxyl groups, and is free of reducing sugars". The lignin was provided by Wageningen University and Research Centre by dr. ing. R. Gosselink and is a purified form of Kraft pine lignin [47].

The Kraft lignin is 97% lignin on dry basis and the remaining 3% is ash. The elemental composition of the lignin was 61.6 wt% C, 5.9 wt% H, 0.74 wt% N, 1.54 wt% S and 30.22 % O. All monomeric units were of G type [47].

The material is a powder similar to ground coffee beans or fine white sand from a particle size perspective, while the color is dark brown. It has a very typical smell of freshly sawn wood with a hint of vanilla.

Figure 2.1: Indulin AT Kraft feedstock

2.2 Ball Milling

The Kraft lignin was milled in a Fritsch Pulverisette, a planetary ball mill. 50 grams of Kraft lignin was loaded together with 5 large zirconium oxide balls and 10 small zirconium oxide balls, as shown in figures 2.2a and 2.2b.

Six different samples were prepared for this research: an unmilled reference sample and five milled samples with varying milling times. The ball milling instructions dictate that every couple of minutes the ball mill has to stop operating and cool down, as a lot of heat is generated during the milling procedure. For this sample preparation, a 2:1 ratio of pause time to milling time was considered. Secondly, all ball milling took place at 450 rpm, which the maximum for this machine. The procedure for the preparation of these samples is shown in table 2.1.

(a) Ball mill container with balls

(b) Fritsch Planetary ball mill

Figure 2.2: Setup of the planetary ball mil

Table 2.1: Overview of samples and milling time

Sample	Total milling time	Milling time	Pause time	Cycles
0_450	0 min	-	-	-
5_450	5 min	5 min	0 min	1
10_450	10 min	5 min	10 min	2
20_450	20 min	4 min	8 min	5
36_450	36 min	3 min	6 min	12
60_450	60 min	3 min	6 min	20

2.3 Catalyst Preparation

A 20-NiMoP on SiO_2 catalyst was prepared according to ref [60–62]. This involves the following procedure: 1.760 g of $Ni(NO_3)_2{\cdot}6H_2O$ and 1.056 g $(NH_4)_6Mo_7O_{24} \cdot 4H_2O$ were dissolved in 25 mL deionized water and deionized water was added up to 30 mL. A solution of 1.582 g of $(NH_4)_2HPO_4$ in 25 mL deionized water was also prepared. The ammonium phosphate dibasic solution was added to the NiMo solution and the former was rinsed with an additional 5 mL of deionized water. The precipitate that was formed was subsequently dissolved with 8 drops of nitric acid. 5.049 g of silicon dioxide (SiO_2) nanopowder (10-20 nm) was added to the solution to obtain a viscous mixture. It was then stirred overnight at a temperature of 80 °C to evaporate the water at 100rpm.

The resulting solid was dried in an oven overnight at 100 °C. Before calcination, the catalyst was ground with mortar and pestle to a fine powder, and subsequently calcined overnight. The calcination process took place for 4 hours at 500 °C with a heating rate of 2 °C per minute, followed by cooling down to room temperature. 6.388 grams of catalyst precursor was obtained.

3.01 grams of the catalyst precursor was reduced under pure hydrogen flow at 300 mL/min (100 mL/min/g) at 650 °C for 2 hours with a heating rate of 5 °C/min. and cooled to room temperature overnight. For passivation, the catalyst was placed under a 99% N_2/1% O_2 atmosphere for 6h.

2.4 Hydrotreatment procedure

2.4.1 Equipment

The reactor used to carry out the HDO was an autoclave batch reactor from Parr Instrument Company rated for 500 °C and 280 bar. It uses a steel reactor of 100 mL that is clamped on with 6 bolts on two interlocking clamps with a carbon seal ring in between the reactor base and the reactor cup. The stirrer was an 80 Watt overhead stirrer (Heidolph RZR2051control) rated for 20 Ncm up to 2000 rpm, with an radial flow impeller. The reactor had two pressure safety valves to relieve excess pressure in case of accidents, an gas inlet connected to a pressurized hydrogen line and an outlet valve.

The temperature was regulated by a PID controller and the heating was done with a heating mantle that also has water cooling tubing inside. The water cooling tubes are attached to the main water line and is used to cool the reactor and quench the reaction after the reaction is done.

Hydrogen is supplied by a hydrogen booster connected to a replaceable

gas tank. The booster was capable of delivering pressurized hydrogen to a maximum of 180 bar in the current configuration. The setup as described is shown in Figure 2.3.

(a) Disassembled setup

(b) Assembled reactor

(c) Hydrogen booster

(d) Control box

Figure 2.3: HDO equipment configuration

2.4.2 Procedure

The procedure of the reaction was performed is based on work of Osorio Velasco et al. [47] and was as follows: The empty reactor and stirrer were weighed an denoted as $m_{reactor,init}$. 15 grams of lignin (lignin intake) and 0.75 grams of catalyst were added to the reactor. The empty reactor had its

seal contact covered with Never-Seez Regular Grade Lubricating Compound to prevent damage to the seal. The reactor was installed and the clamps were tightened diagonally. The reactor was flushed of air by adding 50 bar hydrogen and relieving the pressure three times. Then, the reactor was tested for leakage by increasing the hydrogen pressure to 150 bar and waiting for 10 minutes after the thermocouple measured at RT. If the reactor leaked, the pressure was relieved and the clamps were tightened more.

To start the reaction, the heating mantle was installed and the reactor was filled with 100 bar hydrogen and the inlet valve was closed. The temperature and pressure were noted. The stirring was started at 600 rpm and the control box was set to 400 °C. Upon reaching 100 °C inside the reactor, the stirring was increased to 1200 rpm. The timer for the reaction was started when the temperature of the reactor first hit 400 °C. The reactor tends to overshoot the setpoint but eventually equilibriate at the set temperature. During the reaction, there was no hydrogen added to the reaction vessel. During the heating, the maximum pressure of the vessel reached 175 bar right after reaching the set temperature. During the reaction, the pressure was noted every hour.

The reaction was performed for 2 hours, after which the control box was set to 0 °C, which caused the cooling valve to open and the heating mantle to turn off. The cooling tap was opened and the mantle was cooled down quickly to quench the reaction. The final pressure before cooling down was 10-20 bar lower than maximum recorded pressure. During the cooling procedure, the stirring was turned down to 200 rpm.

Upon reaching ambient temperature in the reactor, the stirring was turned off and the pressure and temperature were denoted again.

2.4.3 Work-up procedure

After the stirring was turned off, the mixture was left to settle for 10 minutes to collect all products in the container. A 3L Tedlar gas bag with propylene fitting was attached to the gas valve and pressure was relieved to fill up the bag. The bag was detached, and more gasses were vented until the pressure gauge reached 10 bars. A syringe with a gas stopper was attached and 60 mL of product gasses were removed for the Gas-GC analysis. The remaining air was vented and the valve was kept open.

The clamps were detached and the reactor was removed from the base. The stirring rod was screwed out and placed in the reactor. As much oil as possible was scraped from the thermostat and of the reactor internals. The reactor and stirrer were weighed and this was denoted as $m_{reactor,after}$.

The liquid was poured out into a 15mL centrifuge tube. Remaining oil

was scraped out into this tube as well. This was centrifuged at 4000 rpm for 20 minutes. The remaining oil in the reactor was washed out with acetone and passed through a filter.

The centrifuged oil forms 3 layers. These layers are, ordered top to bottom: an oil layer, a water layer and an heavy oil/solid paste layer. The top oil and water layer were decanted and weighed and denoted as Lignin oil and Water respectively. The bottom paste could not be poured out but was suspended in acetone and passed through the same filter as before. The acetone solution below the filter was evaporated on air and the filter was left to dry. The solids on the filter were weighed after and written as m_{solid} and the dried acetone solubles was weighed as $m_{residualoil}$. The total oil weight (m_{oil}) was the sum of the lignin oil and the residual oil. Notably, the oil that resulted after evaporating the acetone had a higher density than water, whereas the top oil is lighter than water.

The workup is schematically shown in Figure 2.4.

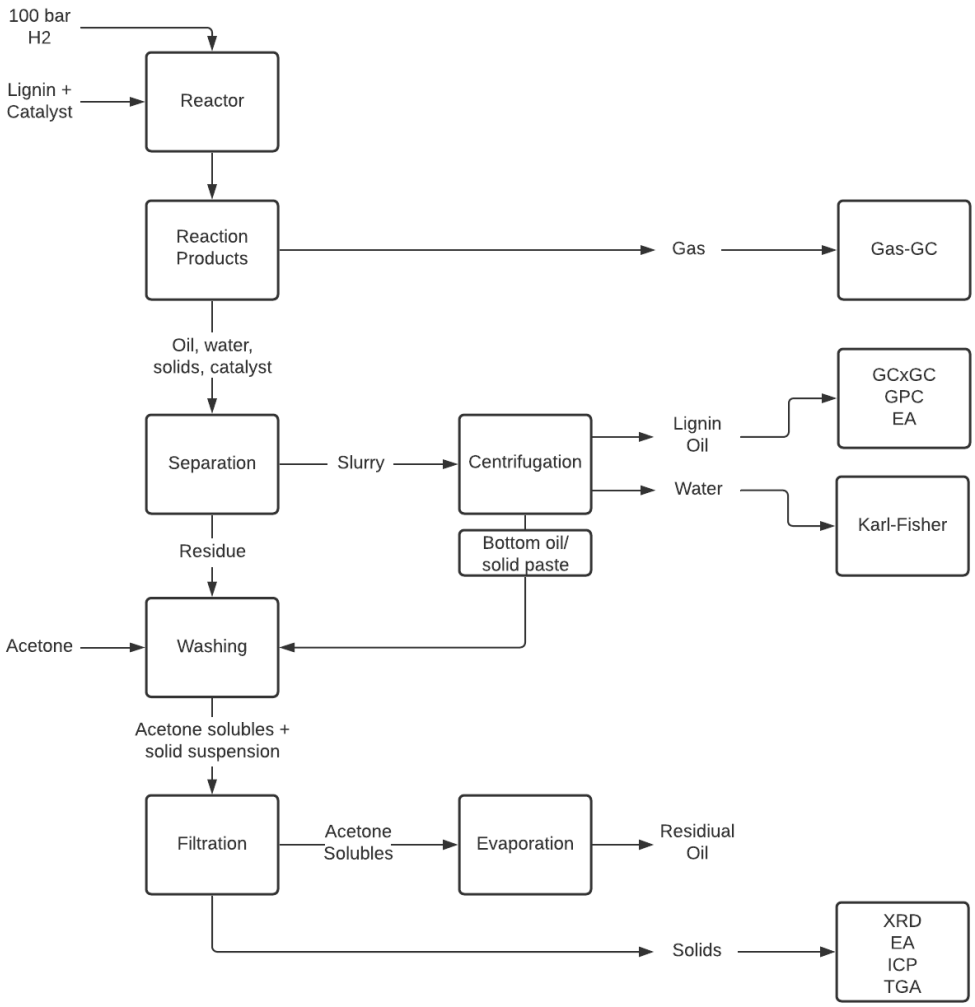

Figure 2.4: Work-up Procedure

2.4.4 Calculations

For each of the 6 different milling times, the HDO experiment was performed twice. The water yield and solid yield are based on measuring the weight, while the oil yield is obtained by the difference in reactor weight before and after reaction, and the water and solid weights. Similarly, the solid yield is the total amount deposited on the filter paper minus the catalyst intake. The gas weight is obtained using the relative concentrations obtained by the Gas-GC and temperature/pressure readings in conjunction with the ideal gas law. The equations for determining the mass balance were as follows:

$$m_{oil}\,(g) = m_{reactor,after}(g) - m_{reactor,init}(g) - m_{water}(g) - m_{solid}(g) \tag{2.1}$$

$$m_{solid}\,(g) = m_{filter,after}\,(g) - m_{filter,init}\,(g) - m_{catalyst}\,(g) \tag{2.2}$$

$$oil\ yield\,(\%) = \frac{m_{oil}}{Lignin\ intake\,(g)} \tag{2.3}$$

$$water\ yield\,(\%) = \frac{m_{water}}{Lignin\ intake\,(g)} \tag{2.4}$$

$$solid\ yield\,(\%) = \frac{m_{solid}}{Lignin\ intake\,(g)} \tag{2.5}$$

$$gas\ yield\,(\%) = \frac{m_{gas}}{Lignin\ intake\,(g)} \tag{2.6}$$

$$mass\ balance\,(\%) = \frac{m_{gas}\,(g) + m_{solid}\,(g) + m_{water}\,(g) + m_{oil}\,(g)}{Lignin\ intake\,(g)} \tag{2.7}$$

2.5 Analytical Techniques

2.5.1 Analytical sieve

To characterize the milled powder and obtain a certain particle size distribution, an analytical sieve was used. 6 trays with a diameter of 10 cm were used with a sieve size of 200, 100, 75, 50, 25 micrometers and a bottom tray. A vibratory plate was used to propagate the process of sieving. The vibratory plate of the analytical sieve was run for 1.5 hours and the different levels of the sieve were weighed to obtain the particle size distribution.

2.5.2 SEM

In addition to the analytical sieve, scanning electron microscopy (SEM) was considered for the measurement of particle size. Using a Philips XL30 Environmental Scanning Electron Microscope (ESEM), images on the micrometer scale of the lignin powder were made. Firstly, a small amount of lignin of three different milling times, 0 minutes, 10 minutes and 60 minutes, was deposited on the sticky, black surface of a carbon sample disc. Compressed air was used to reduce the layer size of the powder to single particles as stacked particles were blown away. This was done to obtain images where particles can be individually distinguished.

The samples were then covered with ZrO_2 and placed into the microscope. Images were created ranging from a 1 mm scale to 10 µm scale (51 to 6000 times magnification), with a scanning voltage of 10 kV.

The goal of the analysis was to obtain a particle size distribution to quantitatively compare and contrast the different milling times on a particle size scale. To obtain this, an area with good dispersion and many fully visible and no stacking of particles in the images was selected and squared off. Then, all well identifiable particles (edges clearly shown, no overlap with the boundary or below other particles) were circled using projected area diameter to obtain a representative sphere as if it was a full sphere. This is relevant as many particles are not complete spheres. These spheres were then measured in pixels and converted to micrometers using the scale. This process is also called optical granulometry. The diameter of the particle was measured in pixels using Paint.NET and converted to µm using the scale of the image.

2.5.3 HSQC

Ball milled lignin and raw lignin were dissolved in deuterated DMSO and NMR was used to obtain a 2D heteronuclear single quantum coherence spectrum to analyze specific types of functional groups to observe changes in chemical structure caused by ball milling. The method was based on literature from Hita and colleagues [63]. 0.2g lignin was dissolved in 0.8g d_6-DMSO The machine of choice was a Bruker Ascend 600 NMR spectrometer and samples were analyzed using a standard pulse sequence HSQC programme with a spectral width of 160 ppm with 4 scans and 512 increments. The data was anaylyzed with MesReNova software.

2.5.4 XRF

The material of the ball mill drum and balls are zirconium oxide, which is an incredibly hard and durable material. As zirconium is a transition metal, it may have catalytic effects if it were present in an HDO setup analogously to other transition metals such as iron, copper, cobalt and more. XRF was used to quantitatively determine if any abrasion occurred during the ball milling and if any zirconium oxide or zirconium was observed in the lignin powder.

2.5.5 GPC

Gel Permeation Chromatography (GPC) was used to identify the molecular weight distribution of a sample. A concentration of 5 mg/ml sample in THF was prepared. The solution was filtered through a teflon filter to remove any insolubles. To that, a drop of toluene was added to serve as a flow marker. The degasser, pump and ALS are part of the Agilent 1100 Series and the detector is a GBC LC 1240 RI detector. For the column, a 3x PLgel Mixed E 3 µm column was used with a linear range of 500 to 25000 Da. The solvent was THF with 2000 ppm stabilized BHT calibrated with a polystyrene standard. Flow rate of THF was 1 mL/min at a 140 bar pressure. The column temperature was 40 °C and a sample of 20 µm was injected at 0.2 wt% concentration. Analysis was done with PSS WinGPC Unity.

2.5.6 Karl Fisher Titration

In order to determine the water content in the oil, a 702 SM Titrino was used for a Karl Fisher titration. The titer was first calibrated using MiliQ water and samples were analyzed in duplo. The titrant used was Hydranal, which is a two-part methanol based titer. The solvent is based on methanol, imidazole and sulphur dioxide and the titrant was Titrant 5 from Hydranal.

2.5.7 XRD

X-Ray Diffraction, or XRD, was used to characterize the crystal structure of fresh and spent catalyst. XRD patterns were collected using a Bruker D8 Advance diffractometer, operating at 40 kV and 40 mA using Cu-Kα radiation (λ=1,5544 Å). Data were collected using a coupled $2\theta/\theta$ configuration, between 2θ values of 5–80 °, with a step size of 0.02 and a scan time of 1.000 s. Analysis was performed in HighScore and known spectra were scored to fit the data.

2.5.8 TGA

Thermogravimetric analysis is used to determine the content of volatiles and the solids' thermal stability in the spent catalyst and solid mixture. 5 mg of substrate is placed in a small cup and heated from 50 to 900 °C at a heating rate of 10 °C/min in a Perkin Elmer TGA 4000. A gas flow of 30 ml/min air was used to evacuate gasses and the weight of the sample was recorded over the full range of temperatures.

2.5.9 EA & ICP

Elemental analysis in the form of EA and ICP were outsourced through the Chemical Engineering department in order to analyze the quantity of different elements. EA was used to determine the C, N and H quantity in lignin oil and acetone oil samples. Oxygen content can be derived by difference. ICP was used to determine the quantity of metals in the spent and fresh catalyst to support XRD data.

2.5.10 BET

The specific surface area and pore properties of 20-NiMoP on SiO_2 catalyst were determined by N_2 physisorption, using a Micromeritics ASAP 2420 system. Before analysis, the sample of approximately 100 mg was subjected to a vacuum at 250 °C for 6 hours to degas the catalyst. The specific surface area was measured using the Brunauer-Emmett-Teller (BET) method at relative pressures (P/P_0) ranging from 0.05 to 0.25 at a temperature of -196 °C (77K, boiling point of molecular nitrogen). The total pore volume was obtained from the single point desorption data at a relative pressure of 0.98. The pore diameter was calculated using the adsorption branch from N_2 isotherm with the Barrett-Joyner-Halenda (BJH) method.

2.5.11 NH_3-TPD

NH_3 Temperature programmed desorption (TPD) was used to quantify the surface acidity of the 20-NiMoP catalyst using a Micrometics AutoChem 2920. Approximately 100 mg of catalyst was placed in the device to calcinate at 550 °C under a He flow of 50 mL/min and subsequently a gas mixture containing 10% NH_3 by volume in He (50 mL/min) was used to saturate the acidic sites of the catalyst surface. After saturation, the catalyst was purged by a He flow (50 mL/min). The desorption measurements were performed in a temperature range of 100 to 700 °C at a heating rate of 10 °C/min.

2.5.12 GCxGC

Two dimensional Gas Chromatography (GCxGC) was used to make a 2D spectrum of the oil composition. 2 different columns in sequence are used to obtain a unique separation profile that allows for analysis and characterization of a large number of similar compounds. The method was based on literature [64]. This method also allows for integration in bulk to obtain relative presence of different fractions (such as alkylphenolics, hydrocarbons, cyclic alkanes, fatty acid methyl esters etc.). A Interscience Trace 2DGC with a custom autosampler were used for this process. Oil was diluted approximately 40x in THF with known quanity of dibuytyl ether (DBE) as internal standard and the modulator was set to alternate at 3 second intervals. The machine used a cryogenic trap system cooled by pressurized CO_2. The injector temperature was set to 280 °C and the oven temperature was 250 °C.

2.5.13 Gas-GC

For the analysis of gasses from the HDO, a Gas-GC was used. The Gas-GC was a 5890 Series II Gas Chromatograph from manufacturer Agilent Technologies (image 2.7). A method was to identify the hydrocarbons up to C_3 (methane, ethane, ethylene, propane, propylene), CO, CO_2 and H_2. A reference gas (18.1 % CO_2, 0.4926 % Ethylene, 1.53 % Ethane, 0.5026 % Propylene, 1.51 % Propane, 20.2 % CH_4, 3.02 % CO, 54.6 % Hydrogen (by difference)) was used to find the relative response factor in order to calculate the concentrations of each of these compounds. For each Gas-GC sample, 60 mL of reactor atmosphere after the reaction was collected. Each reaction had its gas analysed in duplo (30 mL each sample).

Figure 2.5: GPC

Figure 2.6: GCxGC

Figure 2.7: 5890 Series II Gas Chromatograph

Chapter 3

RESULTS AND DISCUSSION

3.1 Ball Milling and Particle Size Distribution

This section will comprise of the comparison between milled and unmilled lignin on a particle level scale. This will contain a visual comparison and a comparison with scanning electron microscopy. Finally, a cumulative particle size distribution for unmilled and two milled samples will be produced. The analytical sieve was unsuitable for the separation of particles, as the particles were too cohesive to separate in a sieve. Drying the Kraft lignin prior to milling also did not allow for sieving.

Visually, there was no difference between the milled samples. Compared to the original Kraft lignin, milled lignin was lighter in color and more cohesive, indicative of a finer powder with smaller particles. Between different milled samples, there was no clear distinguishable difference on color or cohesiveness.

(a) Unmilled lignin (0_450) (b) Milled lignin (20_450)

Figure 3.1: Visual comparison of unmilled and milled Kraft lignin

3.1.1 SEM

The goal of the SEM analysis was to measure the particle size and produce a particle size distribution from a set of particles. Macro overview images of SEM analysis of the three samples with the same scale is shown in Figure 3.2. The complete collection of the SEM imagery are shown in Appendix A.1.

Analyzing the images required clearly differentiable particles. For unmilled lignin, this condition was met at a scale of 500 µm while for milled lignin this was the case at 50 µm. The analysis as set out in section 2.5.2 was performed on two different scales but will be compared nevertheless.

The reasoning behind this is that the much larger particles of unmilled lignin at a very small scale will not give a significant amount of particles in view to create a particle size distribution. On the other hand, the milled lignin has to be measured at lower scale since the particles would be too small to effectively analyse at a larger scale with inaccuracies in the measurement technique.

However, this leaves a minor factor unaccounted for: very small particles which would be observable in 50 µm scale that are invisible at 500 µm scale are unrepresented in the particle size distribution for unmilled lignin. To account for this, unmilled lignin was also analyzed at 50 µm and it was found that the amount of very small particles under 2 µm in unmilled lignin was negligible compared to milled lignin. This is qualitatively shown in Figure 3.3

Comparing the images qualitatively in Figure 3.2, it is seen that unmilled lignin contains many spheres. In contrast to unmilled lignin, milled lignin contains solely fragments. In the milled lignin, there are some particles which are much larger than the rest. This can only be attributed to the fact that not all milling occurs homogeneously. There is a cavity in between the lid and the milling drum where larger particles can remain which get mixed in with the bulk milled lignin after the milling process. These larger particles will not be included in the average particle size, as the frequency of such particles is extremely low and not representative of the milling process.

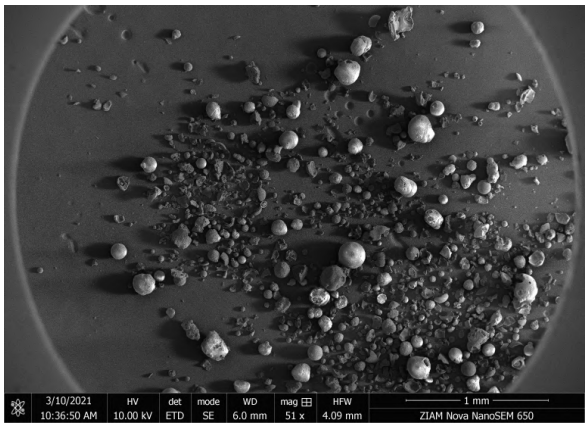

(a) Unmilled lignin analysis (scale=500µm)

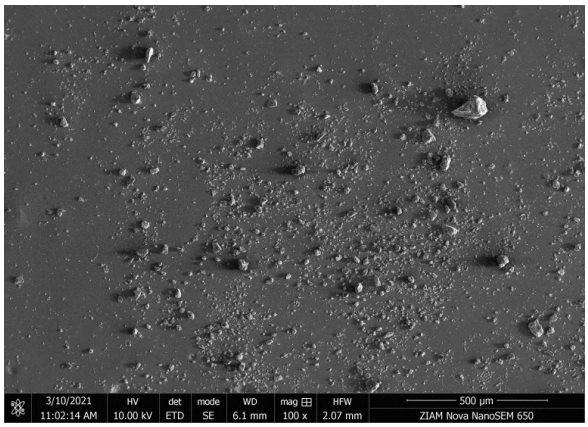

(b) 10 min milled lignin analysis (scale=50µm)

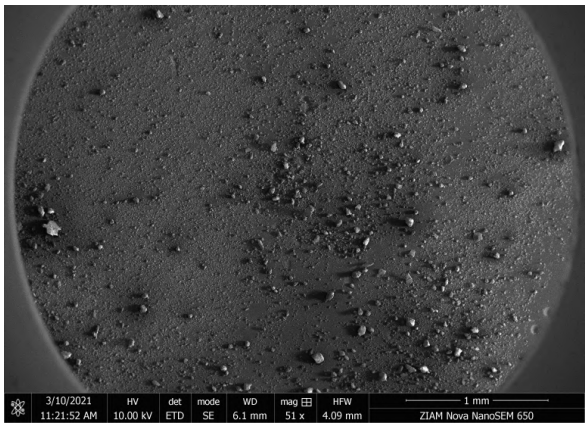

(c) 60 min milled lignin analysis (scale=50µm)

Figure 3.2: Macro SEM images

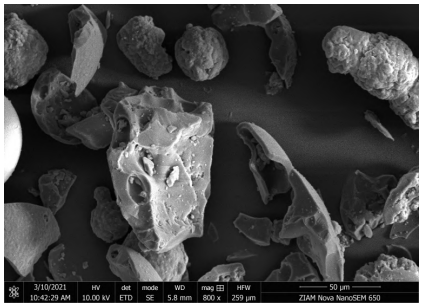

(a) Unmilled lignin (scale=50µm)

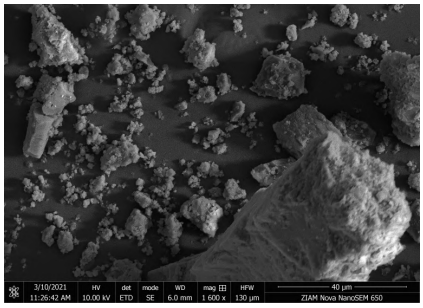

(b) Milled lignin (scale=40µm)

Figure 3.3: Comparison of unmilled and milled lignin at very small scale: qualitative difference between very small (under 2 µm) particles

3.1.2 Particle size distribution

The particles were analyzed with the method described before and the diameter was converted to µm. The particles were grouped in discrete ranges of which the mean diameter was chosen for the particle diameter for the cumulative particle size distribution. The table with all measurements can be found in appendix A.2.

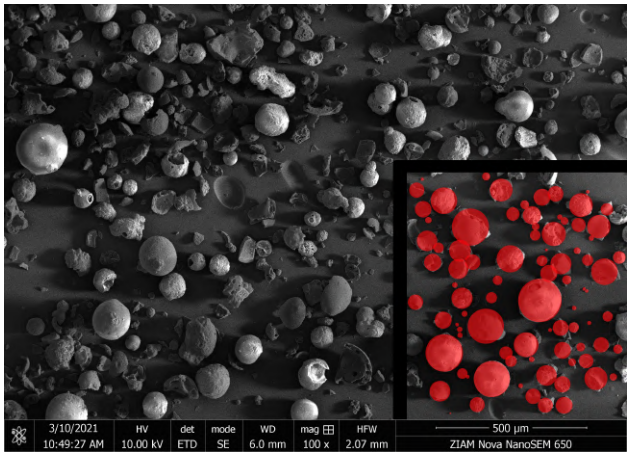

(a) Unmilled lignin analysis (scale=500µm), n=84

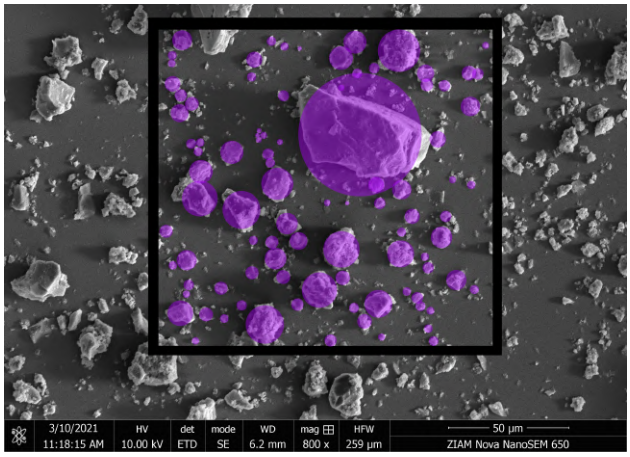

(b) 10 min milled lignin analysis (scale=50µm), n=92

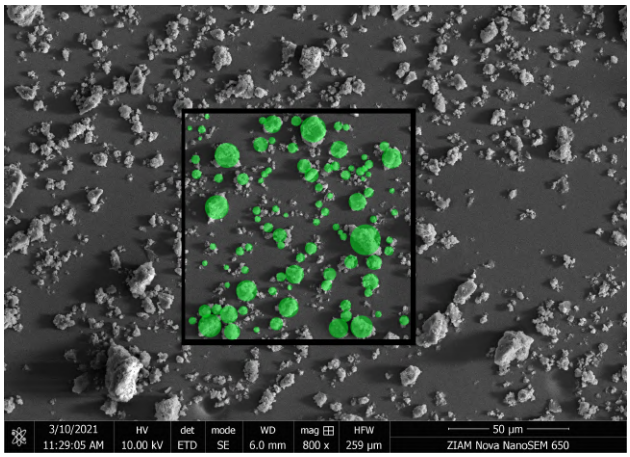

(c) 60 min milled lignin analysis (scale=50µm), n=125

Figure 3.4: Analysed SEM images

The particle size distribution is graphically represented in Figure 3.5. The mean and median particle size is further shown in table 3.1. The difference between milled and unmilled lignin is noticeable, as shown by the mean and median particle diameter: milling for 10 minutes reduces the particle diameter by 88%. Milling for 60 minutes instead reduces particle size by 91% (an additional 27%). The difference between long and short milled lignin of the intensity of 450 rpm is limited. However, the amount of very fine particles between 1-2 µm more than doubled and particles in the range 7-10 µm were diminished by over 75%. In literature, the particle size reduction due to ball milling was also observed [15, 59].

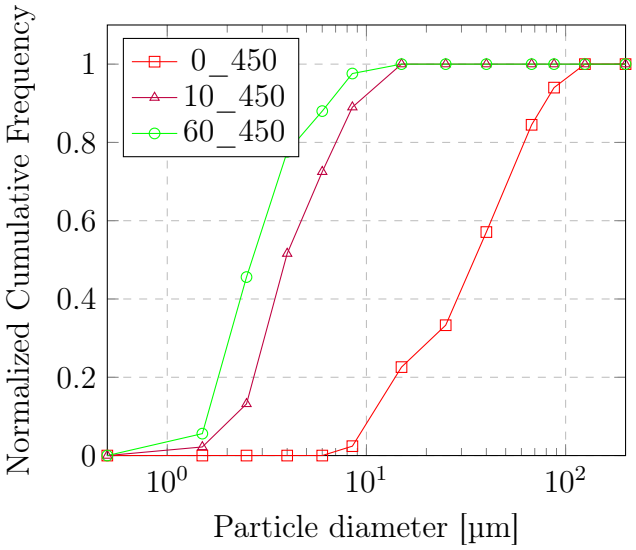

Figure 3.5: Particle Size distribution for unmilled, 10 minute milled and 60 minute milled Kraft lignin

Table 3.1: Mean and median particle diameter

Sample	Mean (µm)	Median (µm)
0_450	46	43
10_450	6.0	4.8
60_450	4.4	3.2

3.2 Catalyst Characterization

In total, 5 different batches of catalyst were used throughout the experiments, each with the same production method. Because of this, slight differences in yields in hydrotreatment can be caused by differences in catalyst activity. For future experiments, this could be improved by mixing multiple smaller batches prior to starting experiments. For the catalyst characterization in this section, the last batch of catalyst was used. The characterization is done using XRD to determine the crystalline structure, BET to determine the surface area and the porous structure, and lastly NH_3-TPD to quanitfy the acidic sites and absorption capacity.

3.2.1 XRD

The XRD spectrum of spent and fresh 20-NiMoP is shown in Figure 3.6. The fresh catalyst contains crystalline structures of $NiMoP_2$, MoP and Ni_2P, while the spent catalyst contains $Na_2(SO_4)_2$ and traces of MoS_2 and MoP. The sulfur originates from the Kraft lignin pulping process and is incorporated into the lignin, while the sodium is a remainder from the sodium hydroxide that is added to the pulping process.

3.2.2 BET

The BET surface area of the catalyst was determined to be 95.4 m^2/g. This value is lower than reported by Osorio Velasco who reported 174 m^2/g [47]. The pore volume was 0.659 cm^3/g catalyst. Hysteresis analysis was also performed [65] and the catalyst behaves as an H3 hysteresis loop with a physisorption isotherm II, see Figure 3.7. This suggests that the catalyst is macroporous or nonporous due to high monolayer-mutlilayer absorption and desporption

3.2.3 NH_3-TPD

The TPD profile shows that the catalyst mainly contains weak/moderate acidic sites as the broad desorption peak is located at low temperatures and centered at 178 °C with adsorption capacity of 543 µmol NH_3/g catalyst. This result is similar, but slightly higher, than the result of Osorio Velasco (411 µmol NH_3/g catalyst) [47], who used a similar catalyst.

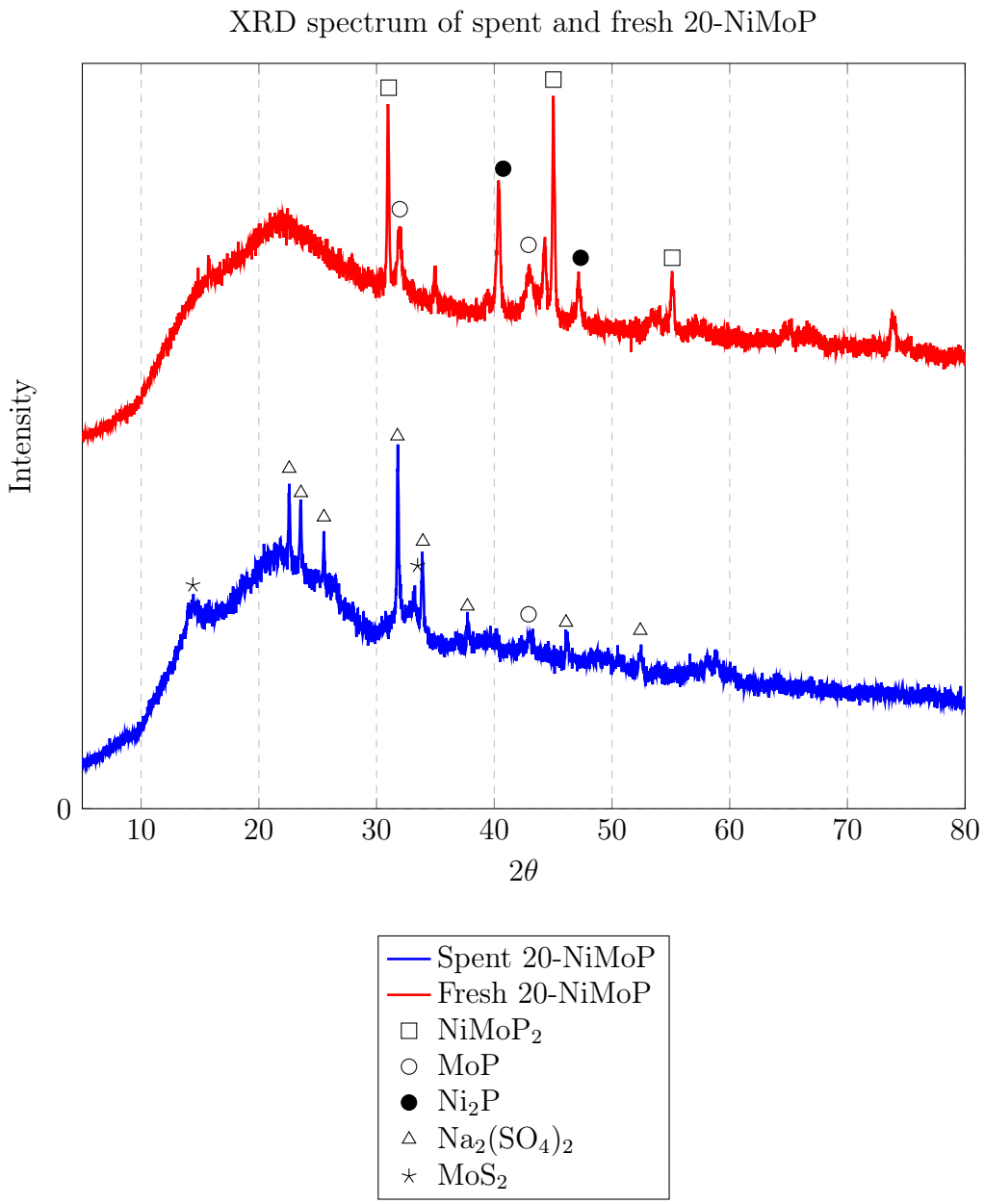

Figure 3.6: XRD of spent catalyst (bottom) and fresh 20-NiMoP catalyst (top) with range 2θ 5°-80°.

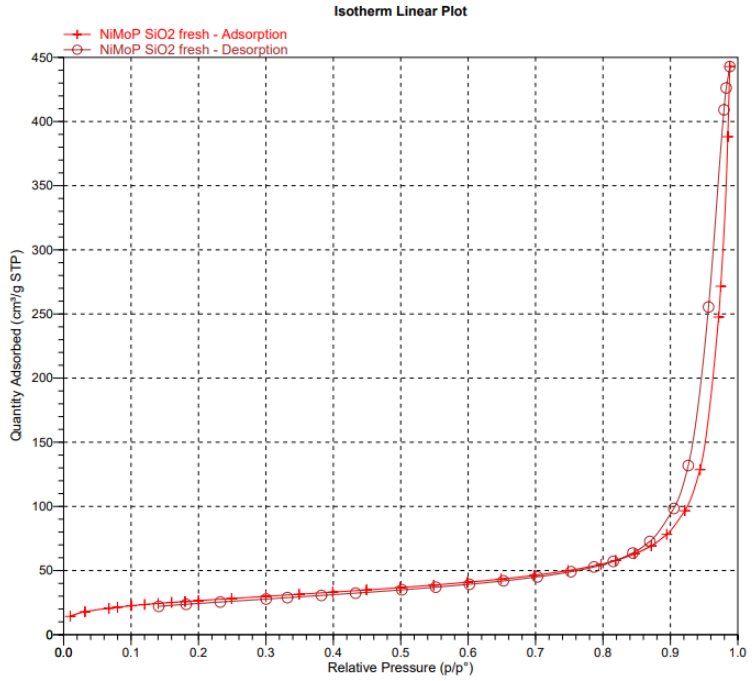

Figure 3.7: BET Hysteresis loop

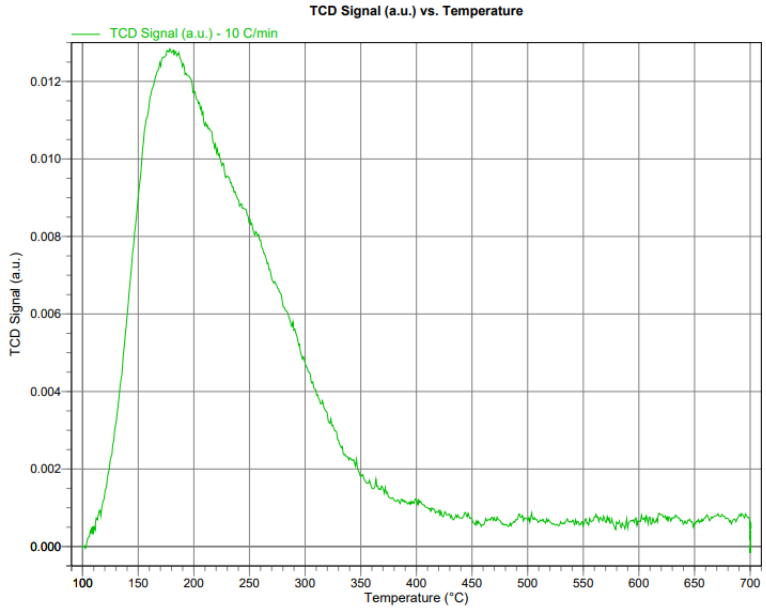

Figure 3.8: TBD Spectrum. Signal (a.u.) versus temperature (°C)

3.3 Chemical Modification due to Ball Milling

In this section, the chemical modification of the Kraft lignin in the ball milling process is discussed. HSQC is used to quantify the functional groups in milled and unmilled lignin, while GPC is used to quantify the reduction or increase in molecular weight from ball milling. Any chemical modification that would occur due to ball milling can later be related to the results of solvent-free catalytic hydrotreatment.

3.3.1 HSQC

HSQC was used to measure the differences in three different linkages between milled and unmilled lignin: β-O-4, β-5_α and β-β_α. The first is one of the weaker C-O bonds, which are expected to break first in mild conditions, and the other two are C-C bonds [63]. The results of the HSQC are visualized in Figure 3.9 and quantified in table 3.3. The data analysis was done by H. Yang

Table 3.3: HSQC Linkage amount [63]

	Linkage amount (per 100 aromatic C9 Units)	
Linkage type	Unmilled Lingin	Milled Lignin
β-O-4	10.41	11.08
β-5_α	3.26	3.37
β-β_α	4.35	5.02

There is a small difference in linkage amount as shown in the table: all linkages are slightly more apparent in the milled lignin, but that is too little difference to be significant. The images show very little structural difference.

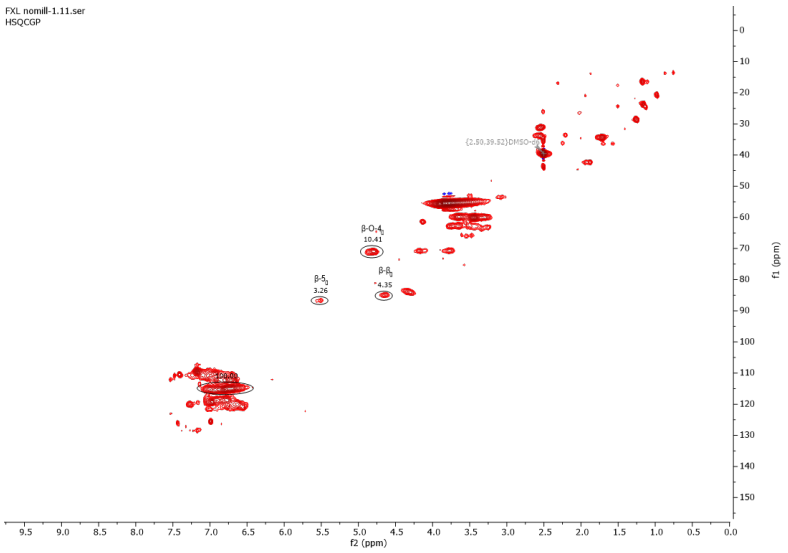

(a) Unmilled lignin HSQC

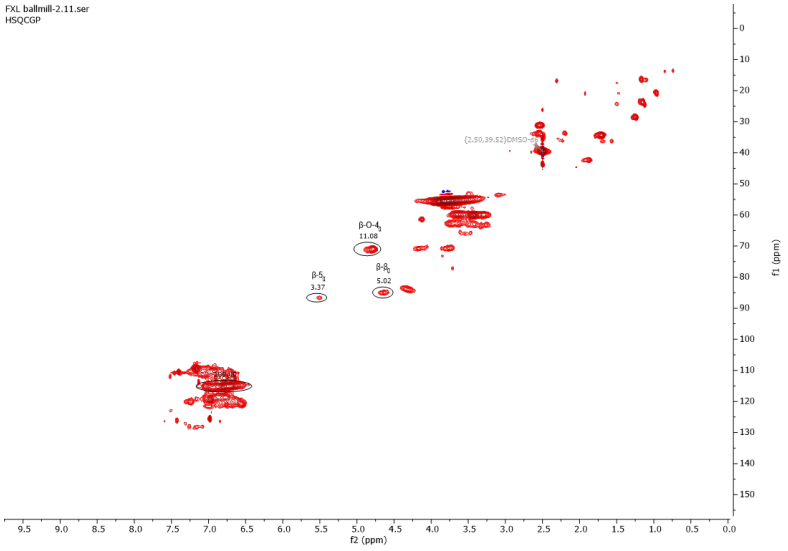

(b) Milled lignin HSQC

Figure 3.9: Comparison of unmilled and milled lignin in HSQC

3.3.2 GPC

GPC of raw Kraft lignin was performed and compared with milled lignin. The results of which can be found in Figure 3.10. The two graphs have been overlayed for easy comparison. As seen from the figure there is no difference in the molecular weight distribution for milled and unmilled lignin. This supports the findings of the HSQC that ball milling does not affect the molecular structure of lignin. Additionally, the average molecular weight of unmilled lignin and milled lignin were 1633 Da and 1548 Da respectively.

Literature findings also support this observation [59], as the required energy to chemically modify the lignin was only achieved at rotational speeds of 2000 rpm (compared to the 450 rpm in present research) and using much smaller balls to increase impacts.

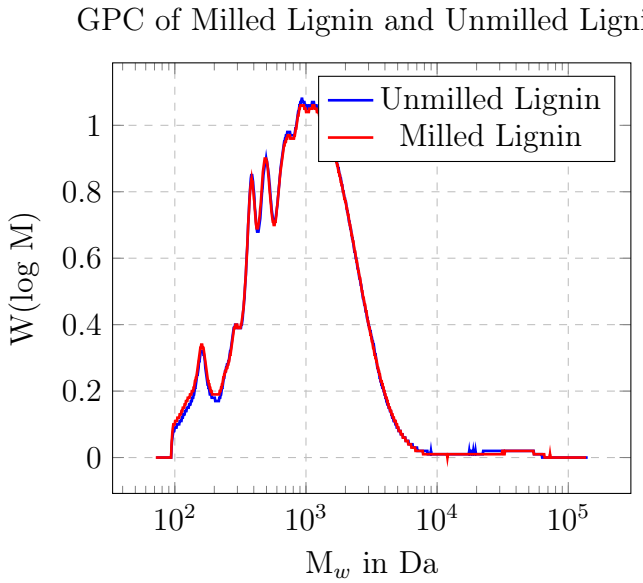

Figure 3.10: GPC Lignin (Red is milled lignin, blue is unmilled lignin)

3.3.3 XRF

XRF was qualitatively used to determine zirconium and zirconium oxide in ball milled lignin and normal lignin. In both samples, no zirconium or zirconium oxide were observed.

3.4 Catalytic hydrotreatment

In total, 22 reactions have been performed, labeled 01 to 22. This includes experiments to get familiar with the setup and the work-up procedure. 12 of these reactions will be considered in the results: a duplo measurement for each milling time. The reactions that are not considered turned out to be leaking gasses, the stirring overloaded or the errors were made in the workup or catalyst production.

3.4.1 Mass balances

To graphically represent the results of the mass balance, the different phases (gas, oil, water, solid) along with the mass balance were averaged over 2 experiments for each milling duration. This is shown in Figure 3.11. The numerical results of each experiment can be found in appendix B.1. Additionally, the oil composition is outlined in figure 3.16. The best duplicated result was obtained at 60 minutes of milling, which had an oil yield on lignin intake of 69.5 %.

As can be seen from the graph, the gas and solid fractions show very consistent results. However, the oil and water along with the mass balance deficit show variations. The main cause for this is that while removing the liquid from the system, part of this gets stuck in the internals of the reactor (pressure gauge tube, thermocouple, etc.). Additionally, during the evaporation stage of the washing with acetone, water and low molecular weight hydrocarbons can evaporate. This in turn lowers the yield of both the water and the oil fraction. This is valid under the assumption that any solids do not remain inside the system, which was checked by filtering the washing solvent (acetone) when cleaning the reactor after the experiment. It showed no significant amount of solids. Additionally, the residue oil layer was more dense than water, while the lignin oil layer was less dense than water.

The gas production is very constant over all reactions as it ranged from 9.9% to 11.7% . The solids show a clear decrease in presence if the lignin is milled prior to HDO: 7.81% is solid before milling, and after miling the solid yield was between 3.2% and 6.8%. These numbers are typical for hydrotreatment of Kraft lignin using NiMoP catalysts [47, 60]. No single experiment using ball milled lignin exceeded the solid yield of any experiment without ball milling.

Mass balance closure is also comparable to literature from Ramesh and colleagues [46], who found mass balance closure between 78% and 96%.

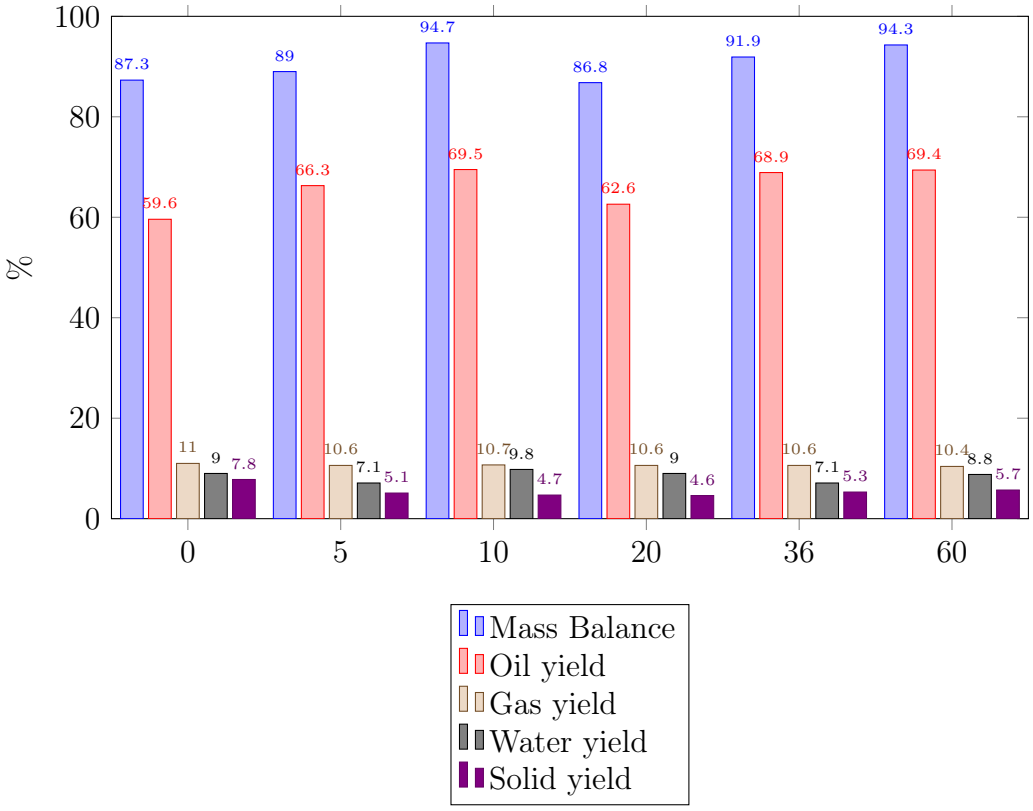

Figure 3.11: Mass balance: Relative weight of different fractions for 6 different conditions. Average of 2 runs. Mass balance and yield on lignin intake

Gas Contents

The main components of the gas phase comprised of H_2 (43.8-53.3%), CH_4 (28.1-35.6%) and CO_2 (8.3-11.4%). Full Gas-GC analysis results can be seen in Appendix C. As there is still a large amount of hydrogen remaining, the reaction was not run until the starvation of hydrogen. CH_4 is likely formed through cracking of methoxy groups and as a product of the Sabatier reaction, which combines CO or CO_2 and H_2 to form methane. This process can be catalyzed by Nickel [66]. CO_2 formation is likely from decarboxylation of organic acids.

Oil Yields

Looking at the oil yield in Figure 3.11, there is also a slight increase in oil yield for ball milled lignin, ranging from 66% [1] to 73 % (averages between 66% and 70 %). The unmilled oil yield averaged at 59.6% and analogously to the solid yield, the milled oil yield was higher than unmilled oil yields. Water yields were relatively constant across all results, but as mentioned before, the mass balance deficit could skew with these results as acetone was used to wash the oil out. This washing could have removed some excess water which subsequently evaporated. In future experiments, a washing step with DCM could improve the mass balance with respect to the water yield.

In cases where the mass balance was high, the increased oil yield from ball milled lignin superseded the results found by J. Osorio Velasco 2021 [47], who found oil yields of 68%. With careful recovery of oil, oil yields of 70 % are achievable.

A possible explanation for the behaviour of decreasing solid production is that on average the particles are more exposed to the hydrogen atmosphere in the heating process under 200 °C. Beyond this temperature, lignin liquidizes and the effects of the reduced particle size should be minimal. This could mean that improved exposure to hydrogen promotes the depolymerization at lower temperature or at the very least have an effect on the equilibrium of depolymerization and repolymerization.

Water Content

In addition to the mass balance shown above, the Karl Fisher titration yielded a 2,7 to 2,9% water yield in the oil for milled lignin, while the unmilled lignin had a water yield of 4,4%. It should be noted that this was merely done for

[1] In the result of 20 min, some oil leaked out skewing the data. For this comparison it is omitted, see also appendix B.1 for the full dataset

the oil of experiment 19 (60_ 450), 21 (0_450), and 22 (10_450). This data is not included in the mass balances shown in Figure 3.11 as the impact it would make is rather small and analysis has not been done for all experiments.

TGA

TGA analysis of the sample showed a small decrease in weight of approximately 2% between 100 and 350 °C. This can be attributed to a small amount of gasses trapped in the catalyst or moisture. Between 350 and 520 °C, 37% of the remaining weight of the sample is gasified. This weight loss can be related to the burning of char and shows an approximate 1/3 of the solid to be char. Upon heating over 600 °C, a small decrease in weight is again observed, which can be attributed to the decomposition of the spent catalyst.

In the experiment, 1.04 g of solids was produced in addition to 0.76 grams of catalyst, which equates to a theoretical char percentage of 58%. It is unlikely that the catalyst gained this much weight during oxidation, so a possible explanation is that carbon is reformed to a more stable compound such as graphite that does not burn off readily and could therefore not be calcined completely. The weight loss profile hints at the regeneration of the spent catalyst, which could be calcined at 550-600 °C to remove the char on it

EA & ICP

At the time of writing, the queued samples for EA and ICP have not yet been analyzed.

3.4.2 GPC of Lignin Oil

The data from the Gel Permeation Chromatography is combined into a single figure as can be seen in Figure 3.13. The main takeaway is that the shapes of all graphs are very similar with a maximum around 145 Da, with the sole difference being an increase in presence of a 200 Da compound for a 36-minute milled lignin reactant.

Weight average molecular weights (M_w) show very similar molecular weights and no clear trends with molecular weights between 321 Da and 390 Da across all samples, as shown in table 3.4.

As seen before, the molecular weight distribution of milled and unmilled lignin does not vary. As such, the molecular weight distributions of both raw lignin and lignin oil can be compared, as seen in Figure 3.14. In line with the literature, the lignin oil has a much lower molecular weight, with a

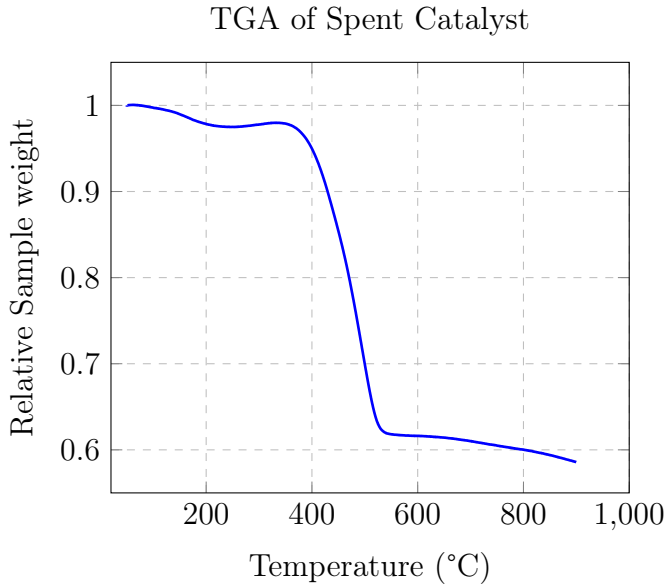

Figure 3.12: TGA of spent catalyst (19-sol) over a range of 50-900 °C, averaged over 2 samples

Table 3.4: Weight average molecular weight in Da, averaged over 2 samples

	M_w (Da)		
	#1	#2	**Average**
0_450	389	388	**389**
5_450	361	333	**347**
10_450	330	321	**326**
20_450	349	355	**353**
36_450	351	370	**361**
60_450	349	388	**369**

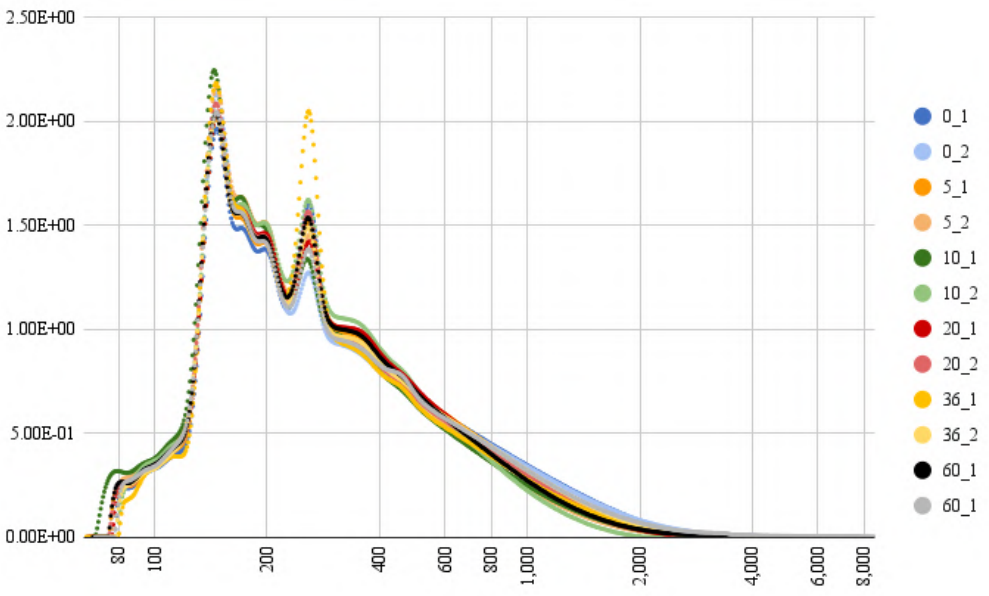

Figure 3.13: GPC of Lignin Oil for different HDO reactions

relative reduction in M_w of 77%. These values are in line with literature [47] (360-450 Da), albeit at the lower end of the spectrum for this catalyst and are lower than the less performing catalyst used by Ramesh [46]. A lower average molecular weight could indicate an increase in monomer content which generally has a lower molecular weight.

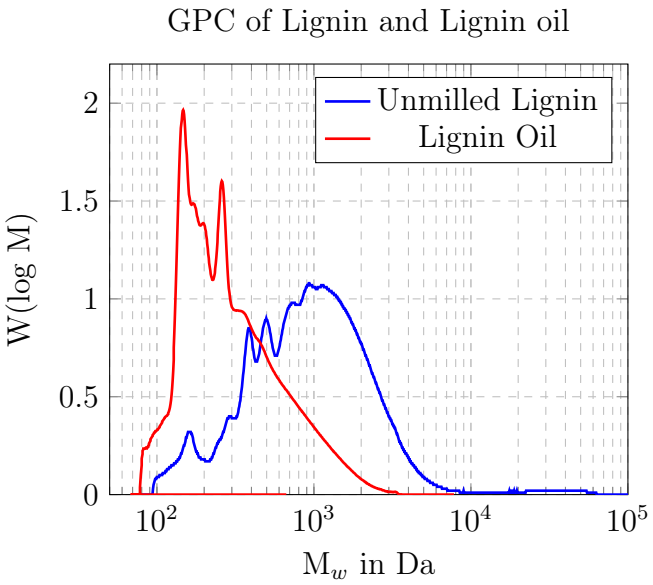

Figure 3.14: GPC of Lignin Oil compared to milled lignin

3.4.3 GCxGC

GCxGC was used to analyze the components in the lignin oil and determine the concentration of monomer as a percentage of the lignin intake. The GCxGC diagram of Experiment 19 is shown in Figure 3.15.

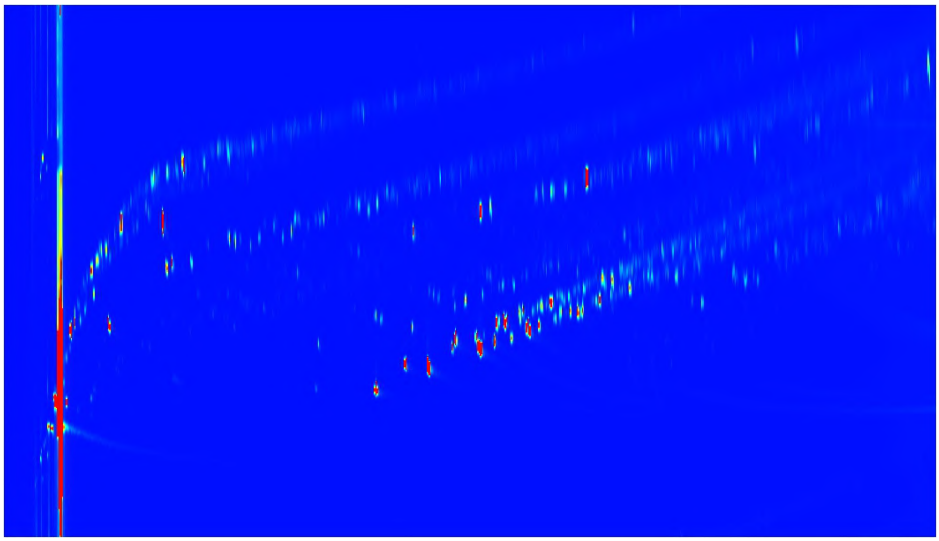

Figure 3.15: GCxGC plot of 60_450. Primary column on horizontal axis, secondary color on vertical axis, intensity by color gradient (red is high, blue is low)

The results of the GCxGC are shown in Table 2.6, which shows identified components, total monomer content and oil yield based on total lignin intake. The results are also graphically shown in Figure 3.16.

The major component of the oils are alkylphenols, with 13.7 wt% yield for unmilled lignin and 14.7-17.6 for milled lignin[2]. The secondary and tertiary products were cycloalkanes and aromatics, which show similar concentrations in oil from unmilled lignin and oil from milled lignin. Lastly, smaller amounts of dihydroxybenzenes, hydrocarbons, ketones, methoxyphenols and naphtalenes are observed, with similar concentrations across all samples. The best duplicated result was obtained at 10 minutes of milling, which had an oil yield on lignin intake of 69.5 %, a monomer yield of 28.2 % and an alkylphenolics yield of 18.6 %.

The milled oil shows a slight increase in phenol concentration, which in turn shows a slight increase in monomer concentration (both on lignin intake). Similarly, the oil yield also increased for milled lignin. Determining the monomer/oil ratio as the amount of monomer as a fraction of the oil yield, it is observed that an increase in monomer count can be attributed to the increase in oil yield as there is no increase of monomer/oil across the experiments. For reference, the relative response factors (RRF) of the

[2]Experiment 16, 20_450 had a leak, therefore oil yield and total monomer content in the sample is lower. For comparisons to unmilled lignin, it will be omitted.

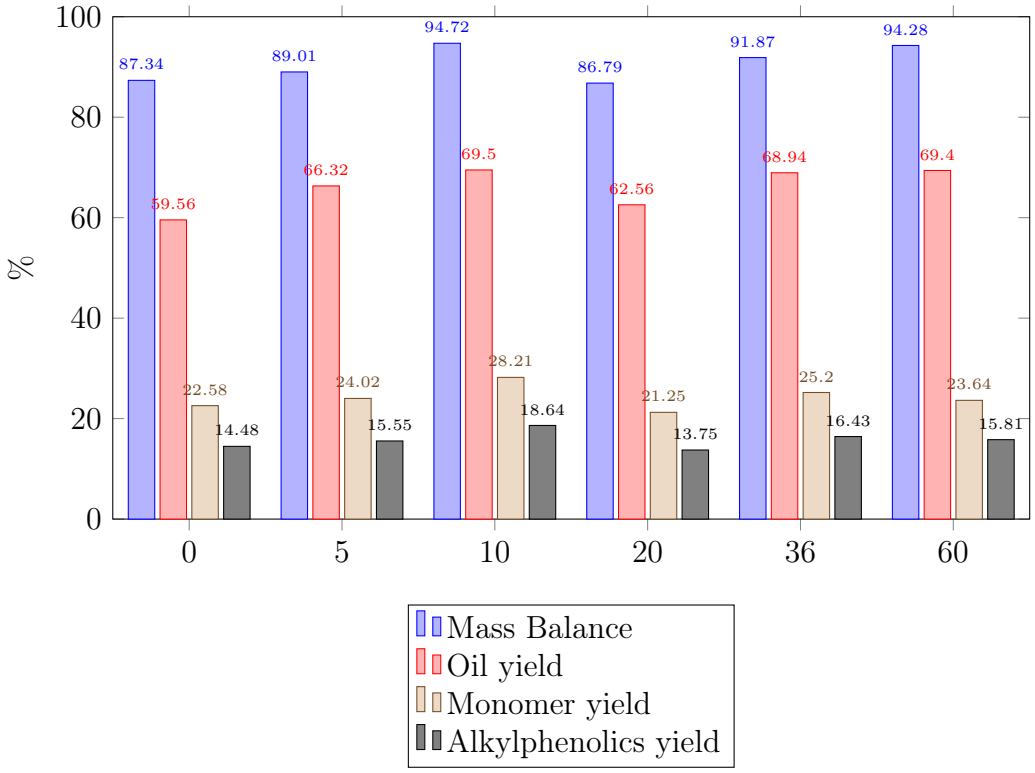

Figure 3.16: Oil composition of 6 different conditions as a percentage of lignin intake. Monomer yield is the sum of Aromatics, Cycloalkanes, dihydroxybenzenes, hydrocarbons, ketones, methoxyphenols, napthalenes and phenols. Alkylphenolics is the sum of phenols and methoxyphenols

Table 3.5: GCxGC comparison of different milling time; Percentage of identified substances on lignin intake

Exp #	450_0 21	450_5 11	450_10 22	450_20 16	450_36 18	450_60 19
Aromatics	2.1	2.3	2.5	1.9	2.2	2.0
Cycloalkanes	2.9	2.9	3.1	2.5	3.1	2.5
Dihydroxybenzenes	0.2	0.1	0.3	0.2	0.3	0.3
Hydrocarbons	1.2	1.1	1.3	1.0	1.1	0.9
Ketones	0.2	0.3	0.3	0.3	0.3	0.3
Methoxyphenols	0.8	0.8	1.1	0.7	0.9	0.7
Naphtalenes	1.5	1.7	2.0	1.6	1.8	1.8
Phenols	13.7	14.7	17.6	13.0	15.6	15.2
Total Monomer	**22.58**	**24.02**	**28.21**	**21.25**	**25.20**	**23.64**
Oil yield	60.61	66.56	71.48	58.70	69.57	65.11
Monomer/oil	0.37	0.36	0.39	0.36	0.36	0.36

components are shown in appendix D as supplied by L. Rohrbach from the analytical department.

Monomer yield is comparable to literature from Ramesh and colleagues [46]. They found a total yield of monomers between 14.8 and 26.4 % depending on catalyst. It should be noted that the catalyst in present research was not investigated by Ramesh.

The monomer yield is low compared to results from Osorio Velasco [47]. She produced monomer yields higher than 50% on lignin intake with a similar catalyst to present research. More careful analysis of the oil would need to be done for present research to rule out any mistakes in the quantification of the monomer count.

Different fractions of the workup (Lignin oil, bottom oil and residual oil) are analyzed through GCxGC for experiment 8 (unmilled lignin) and the results are shown in Table 3.6. It shows that the oil in the bottom and top layer of the workup process is very similar on monomer content. The acetone fraction, which was left to dry on air, shows a lower monomer content. The deficit can be attributed to a decrease in aromatics, such as toluene and benzene, cycloalkanes, such as cyclohexane, and hydrocarbons, such as hexane. These more volatile compounds will evaporate during the acetone evacuation while heavier aromatics, phenols and naphtalenes evaporate to a much lesser degree. A different method of workup can be devised to limit the loss of monomers during the acetone evacuation. Dichloromethane as solvent

can perhaps be used as it evacuates easier than acetone, which would result in less monomers evaporating.

Table 3.6: GCxGC of different fractions of the work-up procedure substances as a percentage on lignin intake (Experiment 8)

	Top	Bottom	Residual
Aromatics	2.3	2.3	1.2
Cycloalkanes	2.9	2.4	0.0
Dihydroxybenzenes	1.0	1.4	1.8
Hydrocarbons	1.2	1.2	0.3
Ketones	0.2	0.3	0.1
Methoxyphenols	0.7	0.8	0.8
Naphtalenes	2.1	1.7	2.2
Phenols	15.0	14.8	15.5
Total Monomer	25.5	24.8	21.9

Chapter 4

CONCLUSIONS

Mechanical pretreatment of Kraft lignin for catalytic hydrotreatment is a simple and effective method to improve the oil and monomer yields while reducing solid residue.

Ball milling Kraft lignin reduces particle size by approximately 90% as a result from SEM analysis. Ball milling for a short time (10 minutes) already reduces particle greatly, and more ball milling up to 60 minutes reduces particle size even more. Analysis of the milled lignin yielded almost no difference between milled and unmilled Kraft lignin on the molecular weight and linkage amount, as determined from GPC and HSQC. Instead, the only observed difference was in the particle size distribution.

Solvent free catalytic hydrotreatment of milled and unmilled lignin produced an 13% increase in oil yield for milled lignin compared to the unmilled counterpart, which was obtained from GCxGC analysis. The monomeric content on the oil yield remained the same. At the same time, the solid residue was decreased by 35%. These improvements are solely caused by particle size as no chemical changes have taken place during ball milling. The difference between long milled and short milled lignin particle size is not reflected in the mass balance results and monomer yields. It turns out that 10 min milling of Kraft lignin is sufficient enough for the increase of oil, monomers, and alkylphenolic yields. The best results that were obtained had an oil yield on lignin intake was 69.5 %, a monomer yield of 28.21 % and an alkylphenolics yield of 18.6 %.

4.1 Recommendations

For further research, ball milling with higher intensity can be investigated. It was shown that chemical modification due to ball milling is possible with

higher intensity in the presence of other reagents [59]. It might be interesting to see the effects of chemical modification on the hydrotreatment. Small balls with higher rotational speed could achieve the suggested effect.

Secondly, temperature dependence has been shown to affect the hydrotreatment results. In this research, the effect of temperature variations was not investigated, but the effect of milling on lignin may be most pronounced at lower temperature. For future research, the effect of temperature variations with ball milled lignin can be examined. This would also be beneficial to the general understanding of lignin depolymerization kinetics.

Bibliography

[1] N. Ahmad and M. R. Zakaria, "Oligosaccharide from hemicellulose," in *Lignocellulose for Future Bioeconomy*, pp. 135–152, Elsevier, 2019.

[2] D. Bajwa, G. Pourhashem, A. Ullah, and S. Bajwa, "A concise review of current lignin production, applications, products and their environmental impact," *Industrial Crops and Products*, vol. 139, p. 111526, Nov. 2019.

[3] R. Abejón, H. Pérez-Acebo, and L. Clavijo, "Alternatives for chemical and biochemical lignin valorization: Hot topics from a bibliometric analysis of the research published during the 2000–2016 period," *Processes*, vol. 6, p. 98, July 2018.

[4] C. Li, X. Zhao, A. Wang, G. W. Huber, and T. Zhang, "Catalytic transformation of lignin for the production of chemicals and fuels," *Chemical Reviews*, vol. 115, pp. 11559–11624, Oct. 2015.

[5] J. Holladay, J. Bozell, J. White, and D. Johnson, *Results of Screening for Potential Candidates from Biorefinery Lignin*, vol. II. U.S. Department of Commerce, 2007.

[6] D. Carpenter, T. L. Westover, S. Czernik, and W. Jablonski, "Biomass feedstocks for renewable fuel production: a review of the impacts of feedstock and pretreatment on the yield and product distribution of fast pyrolysis bio-oils and vapors," *Green Chem.*, vol. 16, no. 2, pp. 384–406, 2014.

[7] C. Biermann, *Handbook of pulping and papermaking.* San Diego: Academic Press, 1996.

[8] Z. Li, "Research on renewable biomass resource-lignin," *Journal of Nanjing Forestry University(Natural Science Edition)*, no. 1, p. 1–7, 2012.

[9] F. Lu and J. Ralph, "Lignin," in *Cereal Straw as a Resource for Sustainable Biomaterials and Biofuels*, pp. 169–207, Elsevier, 2010.

[10] R. Vanholme, K. Morreel, J. Ralph, and W. Boerjan, "Lignin engineering," *Current Opinion in Plant Biology*, vol. 11, pp. 278–285, June 2008.

[11] D. V. Evtuguin, C. P. Neto, A. M. S. Silva, P. M. Domingues, F. M. L. Amado, D. Robert, and O. Faix, "Comprehensive study on the chemical structure of dioxane lignin from PlantationEucalyptus globulusWood," *Journal of Agricultural and Food Chemistry*, vol. 49, pp. 4252–4261, Sept. 2001.

[12] P. C. R. Pinto, E. A. B. da Silva, and A. E. Rodrigues, "Insights into oxidative conversion of lignin to high-added-value phenolic aldehydes," *Industrial & Engineering Chemistry Research*, vol. 50, pp. 741–748, Jan. 2011.

[13] D. Tarasov, M. Leitch, and P. Fatehi, "Lignin–carbohydrate complexes: properties, applications, analyses, and methods of extraction: a review," *Biotechnology for Biofuels*, vol. 11, Sept. 2018.

[14] A. Bjorkman, "Lignin and lignin-carbohydrate complexes," *Industrial & Engineering Chemistry*, vol. 49, no. 9, pp. 1395–1398, 1957.

[15] T. Ikeda, K. Holtman, J. F. Kadla, H. min Chang, and H. Jameel, "Studies on the effect of ball milling on lignin structure using a modified DFRC method," *Journal of Agricultural and Food Chemistry*, vol. 50, pp. 129–135, Jan. 2002.

[16] F. E. Brauns, "Native lignin - i. its isolation and methylation," *Journal of the American Chemical Society*, vol. 61, no. 8, pp. 2120–2127, 1939.

[17] H. min Chang, E. B. Cowling, and W. Brown, "Comparative studies on cellulolytic enzyme lignin and milled wood lignin of sweetgum and spruce," *Holzforschung*, vol. 29, pp. 153–159, Jan. 1975.

[18] G. D. Whiting P., "The morphological origin of milled wood lignin [picea mariana].," *Svensk Papperstidning*, vol. 84, pp. 120–122, 1981.

[19] H. Chen, "Lignocellulose biorefinery feedstock engineering," in *Lignocellulose Biorefinery Engineering*, pp. 37–86, Elsevier, 2015.

[20] A. VAN TRAN, "Effect of cooking temperature on kraft pulping of hardwood," *Tappi Journal*, vol. 1, pp. 13–19, 06 2002.

[21] J. Gierer, "Chemical aspects of kraft pulping," *Wood Science and Technology*, vol. 14, no. 4, pp. 241–266, 1980.

[22] A. Rodríguez, R. Sánchez, A. Requejo, and A. Ferrer, "Feasibility of rice straw as a raw material for the production of soda cellulose pulp," *Journal of Cleaner Production*, vol. 18, pp. 1084–1091, July 2010.

[23] E. Melro, A. Filipe, D. Sousa, A. J. Valente, A. Romano, F. E. Antunes, and B. Medronho, "Dissolution of kraft lignin in alkaline solutions," *International Journal of Biological Macromolecules*, vol. 148, pp. 688–695, Apr. 2020.

[24] T. McDonough, "The chemistry of organosolv delignification," *Inst. Paper sci. Technology*, vol. 76, p. 186–193, oct 1993.

[25] T. Li and S. Takkellapati, "The current and emerging sources of technical lignins and their applications," *Biofuels, Bioproducts and Biorefining*, vol. 12, pp. 756–787, July 2018.

[26] D. S. Zijlstra, C. W. Lahive, C. A. Analbers, M. B. Figueirêdo, Z. Wang, C. S. Lancefield, and P. J. Deuss, "Mild organosolv lignin extraction with alcohols: The importance of benzylic alkoxylation," *ACS Sustainable Chemistry & Engineering*, vol. 8, pp. 5119–5131, Mar. 2020.

[27] P. de Wild; W.J.J. Huijgen; R. van der Linden; H. den Uil; J. Snelders (KU Leuven); B. Benjelloun-Mlayah (CIMV), "Organosolv fractionation of lignocellulosic biomass for an integrated biorefinery," *NPT Procestechnologie*, vol. 1, pp. 10–11, Feb. 2015.

[28] S. Constant, H. L. J. Wienk, A. E. Frissen, P. de Peinder, R. Boelens, D. S. van Es, R. J. H. Grisel, B. M. Weckhuysen, W. J. J. Huijgen, R. J. A. Gosselink, and P. C. A. Bruijnincx, "New insights into the structure and composition of technical lignins: a comparative characterisation study," *Green Chemistry*, vol. 18, no. 9, pp. 2651–2665, 2016.

[29] A. Tagami, *Towards molecular weight-dependent uses of kraft lignin*. Stockholm: KTH Royal Institute of Technology, 2018.

[30] J. Becker and C. Wittmann, "A field of dreams: Lignin valorization into chemicals, materials, fuels, and health-care products," *Biotechnology Advances*, vol. 37, p. 107360, Nov. 2019.

[31] A. R. Ardiyanti, M. V. Bykova, S. A. Khromova, W. Yin, R. H. Venderbosch, V. A. Yakovlev, and H. J. Heeres, "Ni-based catalysts for the hydrotreatment of fast pyrolysis oil," *Energy & Fuels*, vol. 30, pp. 1544–1554, Jan. 2016.

[32] J. bao Huang, S. bin Wu, H. Cheng, M. Lei, J. jin Liang, and H. Tong, "Theoretical study of bond dissociation energies for lignin model compounds," *Journal of Fuel Chemistry and Technology*, vol. 43, pp. 429–436, Apr. 2015.

[33] M. Kosa, H. Ben, H. Theliander, and A. J. Ragauskas, "Pyrolysis oils from CO2 precipitated kraft lignin," *Green Chemistry*, vol. 13, no. 11, p. 3196, 2011.

[34] Z. Ma, E. Troussard, and J. A. van Bokhoven, "Controlling the selectivity to chemicals from lignin via catalytic fast pyrolysis," *Applied Catalysis A: General*, vol. 423-424, pp. 130–136, May 2012.

[35] I. T. Ghampson, C. Sepúlveda, R. Garcia, J. G. Fierro, N. Escalona, and W. J. DeSisto, "Comparison of alumina- and SBA-15-supported molybdenum nitride catalysts for hydrodeoxygenation of guaiacol," *Applied Catalysis A: General*, vol. 435-436, pp. 51–60, Sept. 2012.

[36] C. Li, M. Zheng, A. Wang, and T. Zhang, "One-pot catalytic hydrocracking of raw woody biomass into chemicals over supported carbide catalysts: simultaneous conversion of cellulose, hemicellulose and lignin," *Energy Environ. Sci.*, vol. 5, no. 4, pp. 6383–6390, 2012.

[37] J. Zhang, J. Teo, X. Chen, H. Asakura, T. Tanaka, K. Teramura, and N. Yan, "A series of NiM (m = ru, rh, and pd) bimetallic catalysts for effective lignin hydrogenolysis in water," *ACS Catalysis*, vol. 4, pp. 1574–1583, Apr. 2014.

[38] J. Zhang, H. Asakura, J. van Rijn, J. Yang, P. Duchesne, B. Zhang, X. Chen, P. Zhang, M. Saeys, and N. Yan, "Highly efficient, NiAu-catalyzed hydrogenolysis of lignin into phenolic chemicals," *Green Chem.*, vol. 16, no. 5, pp. 2432–2437, 2014.

[39] Q. Song, F. Wang, and J. Xu, "Hydrogenolysis of lignosulfonate into phenols over heterogeneous nickel catalysts," *Chemical Communications*, vol. 48, no. 56, p. 7019, 2012.

[40] Y. Romero, F. Richard, and S. Brunet, "Hydrodeoxygenation of 2-ethylphenol as a model compound of bio-crude over sulfided mo-based catalysts: Promoting effect and reaction mechanism," *Applied Catalysis B: Environmental*, vol. 98, pp. 213–223, Aug. 2010.

[41] Y. Romero, F. Richard, Y. Renème, and S. Brunet, "Hydrodeoxygenation of benzofuran and its oxygenated derivatives (2, 3-dihydrobenzofuran and 2-ethylphenol) over NiMoP/al2o3 catalyst," *Applied Catalysis A: General*, vol. 353, pp. 46–53, Jan. 2009.

[42] V. M. L. Whiffen and K. J. Smith, "Hydrodeoxygenation of 4-methylphenol over unsupported MoP, MoS2, and MoOxCatalysts†," *Energy & Fuels*, vol. 24, pp. 4728–4737, Sept. 2010.

[43] H. Topsoe, B. Clausen, and F. Massoth, "A review of: "hydrotreating catalysis science and technology"," *Fuel Science and Technology International*, vol. 14, pp. 1465–1465, Nov. 1996.

[44] V. N. Bui, D. Laurenti, P. Delichère, and C. Geantet, "Hydrodeoxygenation of guaiacol," *Applied Catalysis B: Environmental*, vol. 101, pp. 246–255, Jan. 2011.

[45] V. N. Bui, D. Laurenti, P. Afanasiev, and C. Geantet, "Hydrodeoxygenation of guaiacol with CoMo catalysts. part i: Promoting effect of cobalt on HDO selectivity and activity," *Applied Catalysis B: Environmental*, vol. 101, pp. 239–245, Jan. 2011.

[46] C. R. Kumar, N. Anand, A. Kloekhorst, C. Cannilla, G. Bonura, F. Frusteri, K. Barta, and H. J. Heeres, "Solvent free depolymerization of kraft lignin to alkyl-phenolics using supported NiMo and CoMo catalysts," *Green Chemistry*, vol. 17, no. 11, pp. 4921–4930, 2015.

[47] J. O. Velasco, I. van der Linden, P. J. Deuss, and H. J. Heeres, "Efficient depolymerization of lignins to alkylphenols using phosphided NiMo catalysts," *Catalysis Science & Technology*, vol. 11, no. 15, pp. 5158–5170, 2021.

[48] W. He, W. Gao, and P. Fatehi, "Oxidation of kraft lignin with hydrogen peroxide and its application as a dispersant for kaolin suspensions," *ACS Sustainable Chemistry & Engineering*, vol. 5, pp. 10597–10605, Oct. 2017.

[49] T. P. Schultz and M. C. Templeton, "Proposed mechanism for the nitrobenzene oxidation of lignin," *Holzforschung*, vol. 40, pp. 93–97, Jan. 1986.

[50] R. Isha and P. T. Williams, "Pyrolysis-gasification of agriculture biomass wastes for hydrogen production," *Journal of the Energy Institute*, vol. 84, p. 80–87, May 2011.

[51] A. Yamaguchi, N. Hiyoshi, O. Sato, and M. Shirai, "Gasification of organosolv-lignin over charcoal supported noble metal salt catalysts in supercritical water," *Topics in Catalysis*, vol. 55, pp. 889–896, July 2012.

[52] G. P. V. D. Laan and A. A. C. M. Beenackers, "Kinetics and selectivity of the fischer–tropsch synthesis: A literature review," *Catalysis Reviews*, vol. 41, pp. 255–318, Jan. 1999.

[53] R. D. Cortright, R. R. Davda, and J. A. Dumesic, "Hydrogen from catalytic reforming of biomass-derived hydrocarbons in liquid water," *Nature*, vol. 418, pp. 964–967, Aug. 2002.

[54] A. Yamaguchi, N. Mimura, M. Shirai, and O. Sato, "Bond cleavage of lignin model compounds into aromatic monomers using supported metal catalysts in supercritical water," *Scientific Reports*, vol. 7, Apr. 2017.

[55] Z. Yuan, S. Cheng, M. Leitch, and C. C. Xu, "Hydrolytic degradation of alkaline lignin in hot-compressed water and ethanol," *Bioresource Technology*, vol. 101, pp. 9308–9313, Dec. 2010.

[56] J.-M. Lavoie, W. Baré, and M. Bilodeau, "Depolymerization of steam-treated lignin for the production of green chemicals," *Bioresource Technology*, vol. 102, pp. 4917–4920, Apr. 2011.

[57] X. Xian, S. Wu, W. Wei, and F. Zhang, "Pretreatment of kraft lignin by deep eutectic solvent and its utilization in preparation of lignin-based phenolic formaldehyde adhesive," *BioResources*, vol. 16, no. 2, pp. 3103–3120, 2021.

[58] Y. Qu, H. Luo, H. Li, and J. Xu, "Comparison on structural modification of industrial lignin by wet ball milling and ionic liquid pretreatment," *Biotechnology Reports*, vol. 6, pp. 1–7, June 2015.

[59] M. Kandula, T. Schwenke, S. Friebel, and T. Salthammer, "Effect of ball milling on lignin polyesterification with ϵ-caprolactone:," *Holzforschung*, vol. 69, no. 3, pp. 297–302, 2015.

[60] R. K. Chowdari, S. Agarwal, and H. J. Heeres, "Hydrotreatment of kraft lignin to alkylphenolics and aromatics using ni, mo, and w phosphides supported on activated carbon," *ACS Sustainable Chemistry & Engineering*, vol. 7, pp. 2044–2055, Dec. 2018.

[61] P. Yang, H. Kobayashi, K. Hara, and A. Fukuoka, "Phase change of nickel phosphide catalysts in the conversion of cellulose into sorbitol," *ChemSusChem*, vol. 5, pp. 920–926, Apr. 2012.

[62] R. H. Bowker, B. Ilic, B. A. Carrillo, M. A. Reynolds, B. D. Murray, and M. E. Bussell, "Carbazole hydrodenitrogenation over nickel phosphide and ni-rich bimetallic phosphide catalysts," *Applied Catalysis A: General*, vol. 482, pp. 221–230, July 2014.

[63] I. Hita, H. Heeres, and P. Deuss, "Insight into structure-reactivity relationships for the iron-catalyzed hydrotreatment of technical lignins," *Bioresource Technology*, vol. 267, pp. 93–101, Nov. 2018.

[64] A. Kloekhorst, *Biobased chemicals from lignin.* PhD thesis, University of Groningen, 2015.

[65] M. Thommes, K. Kaneko, A. V. Neimark, J. P. Olivier, F. Rodriguez-Reinoso, J. Rouquerol, and K. S. Sing, "Physisorption of gases, with special reference to the evaluation of surface area and pore size distribution (IUPAC technical report)," *Pure and Applied Chemistry*, vol. 87, pp. 1051–1069, Oct. 2015.

[66] I. S. Pieta, A. Lewalska-Graczyk, P. Kowalik, K. Antoniak-Jurak, M. Krysa, A. Sroka-Bartnicka, A. Gajek, W. Lisowski, D. Mrdenovic, P. Pieta, R. Nowakowski, A. Lew, and E. M. Serwicka, "CO_2 hydrogenation to methane over Ni-catalysts: The effect of support and vanadia promoting," *Catalysts*, vol. 11, p. 433, Mar. 2021.

Appendices

Appendix A

SEM

A.1 SEM Images

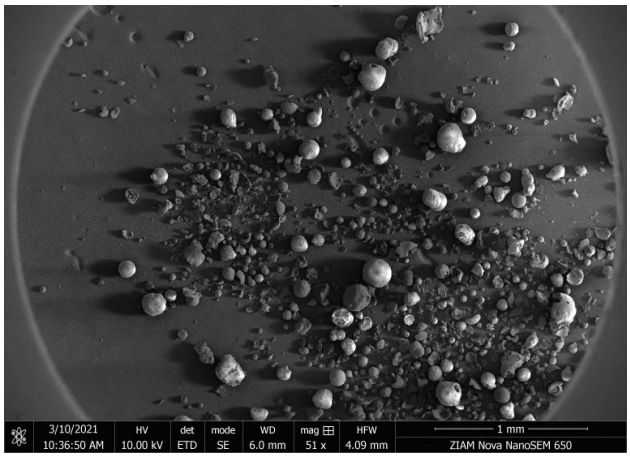

(a) 0_450 Image 1

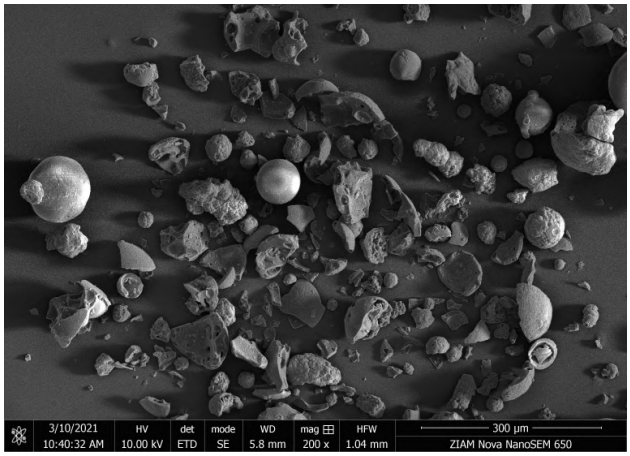

(b) 0_450 Image 2

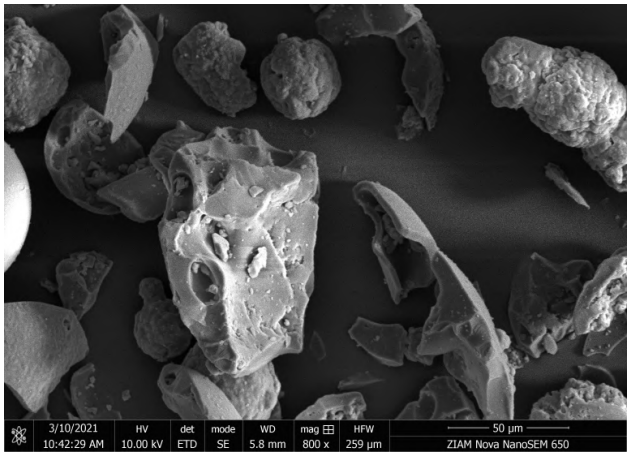

(c) 0_450 Image 3

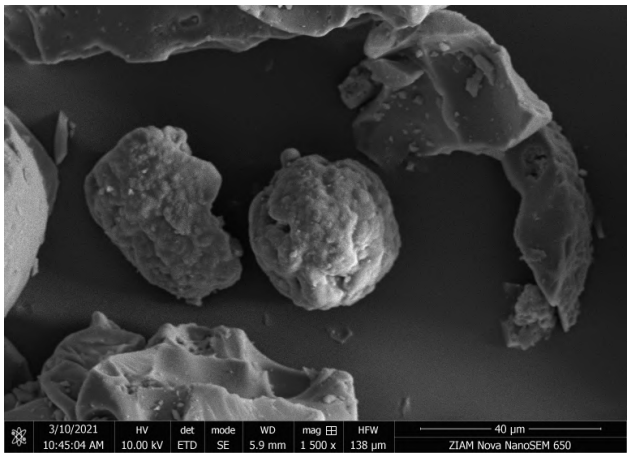

(d) 0_450 Image 4

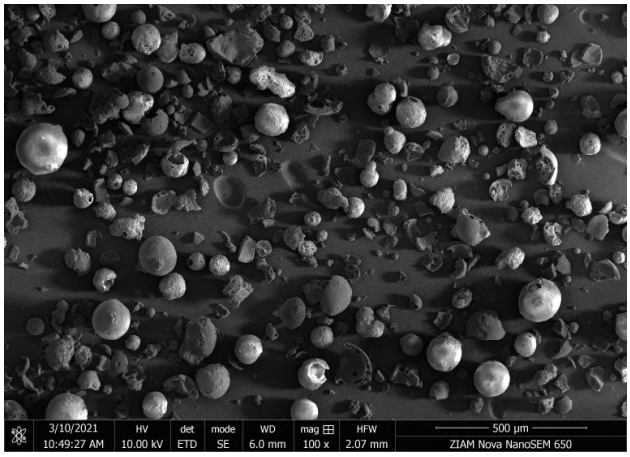

(e) 0_450 Image 5

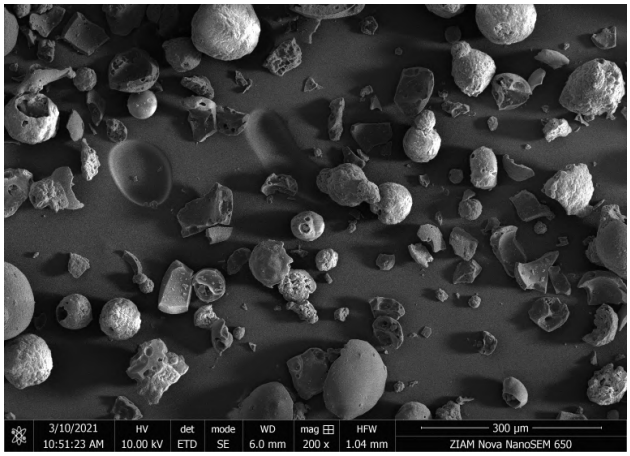

(f) 0_450 Image 6

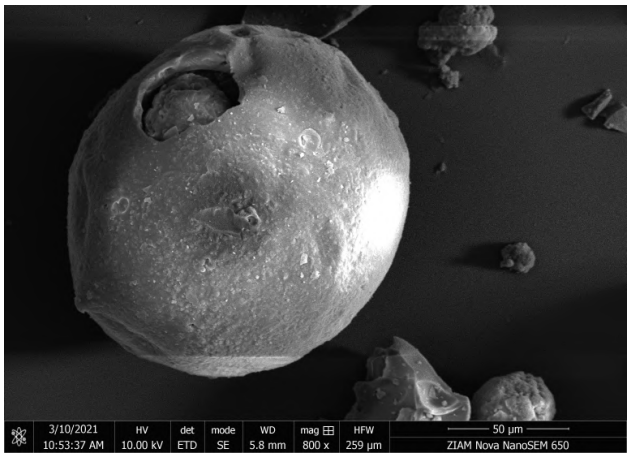

(g) 0_450 Image 7

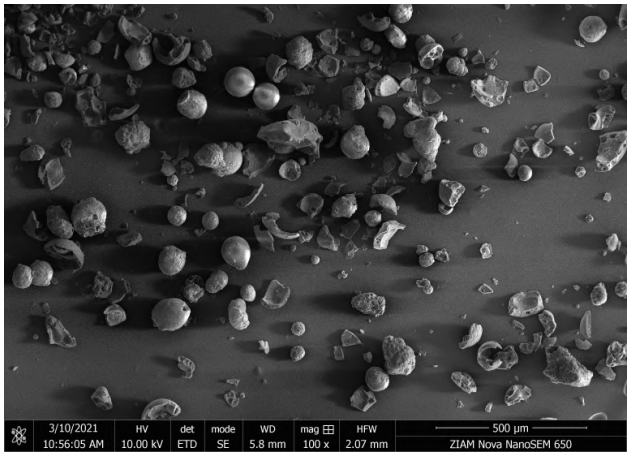

(h) 0_450 Image 8

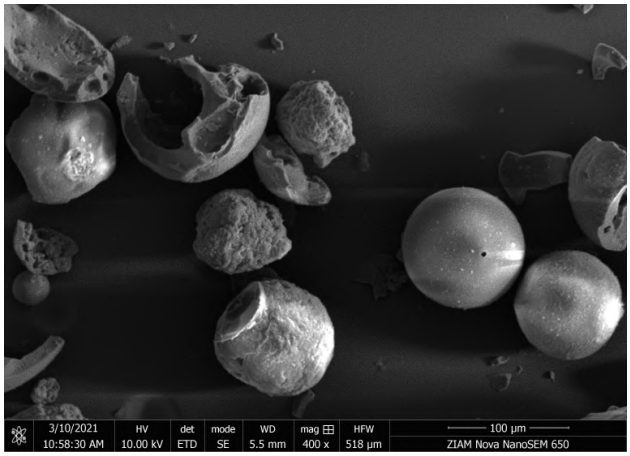

(i) 0_450 Image 9

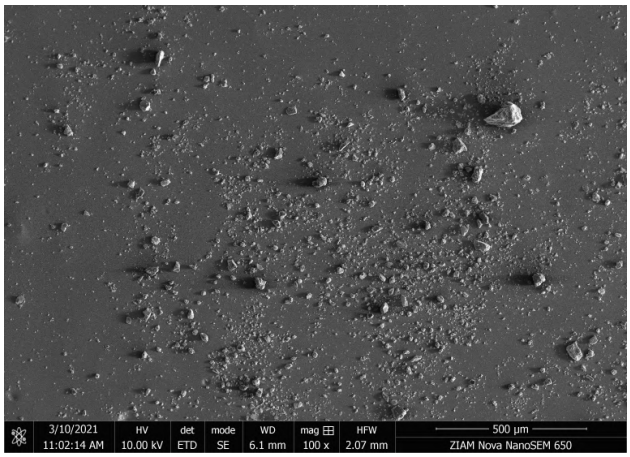

(j) 10_450 Image 1

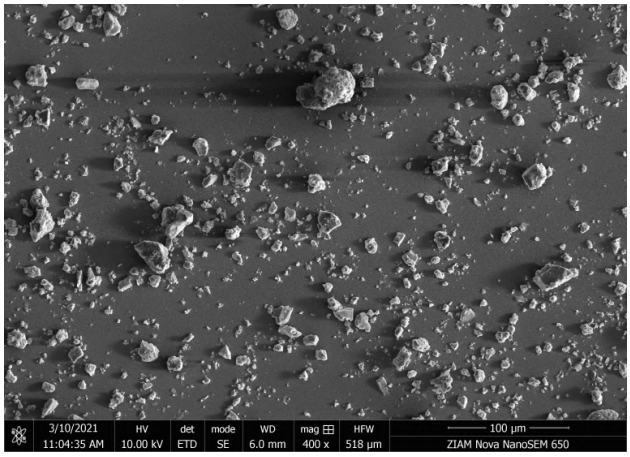

(k) 10_450 Image 2

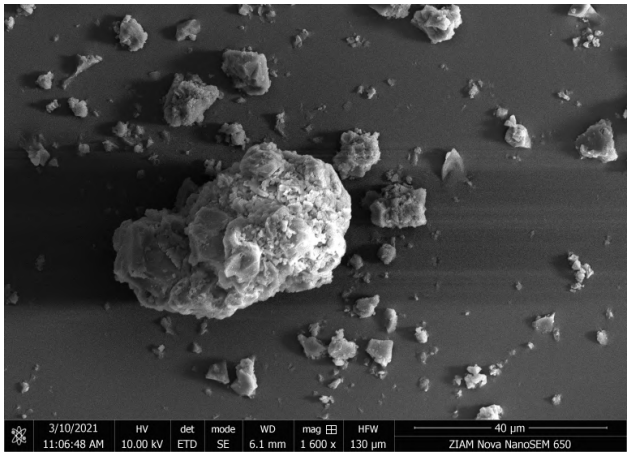

(l) 10_450 Image 3

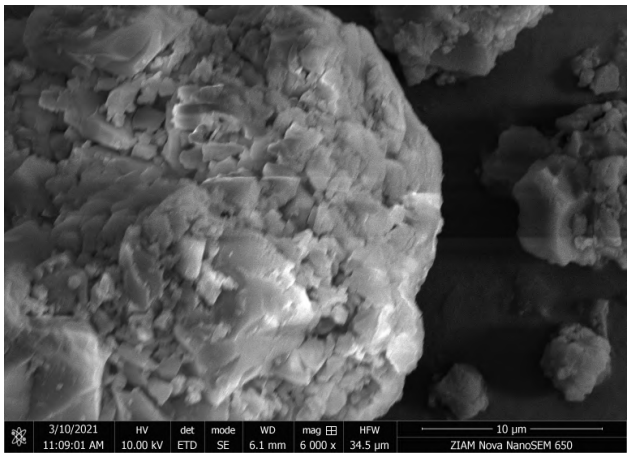

(m) 10_450 Image 4

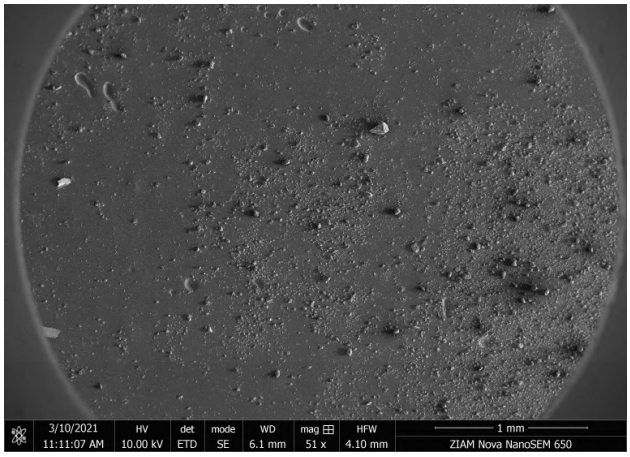

(n) 10_450 Image 5

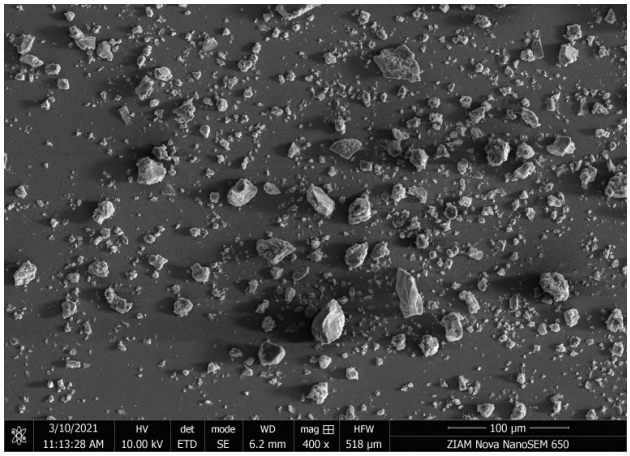

(o) 10_450 Image 6

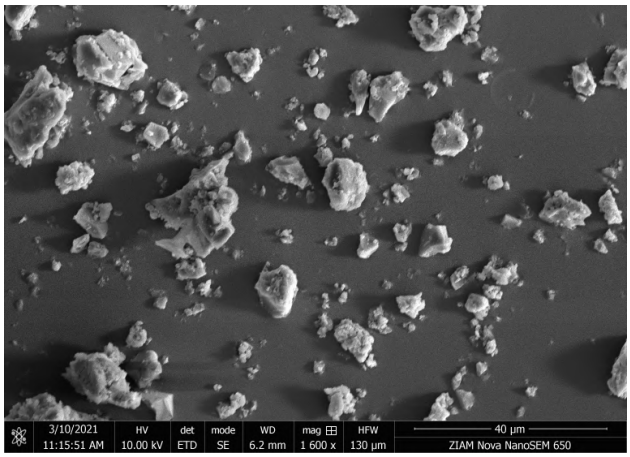

(p) 10_450 Image 7

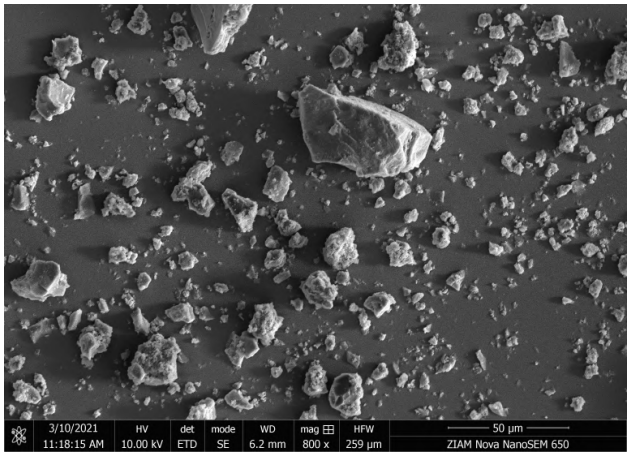

(q) 10_450 Image 8

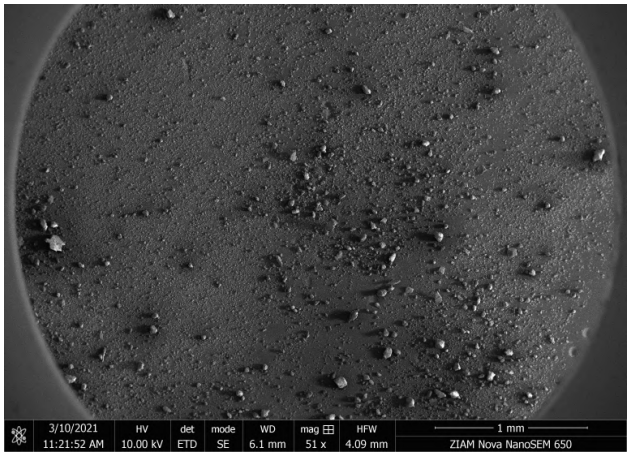

(r) 60_450 Image 1

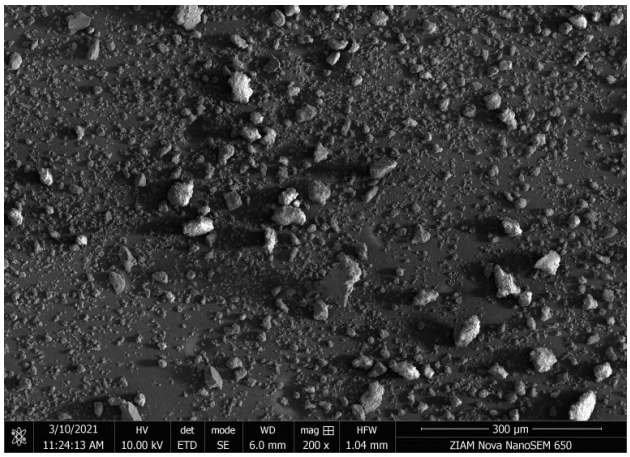

(s) 60_450 Image 2

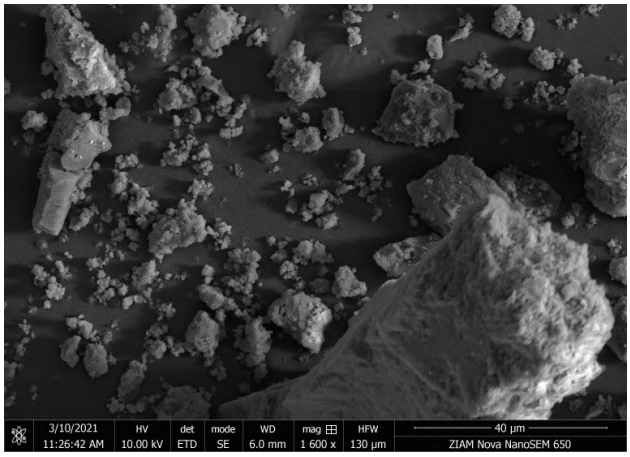

(t) 60_450 Image 3

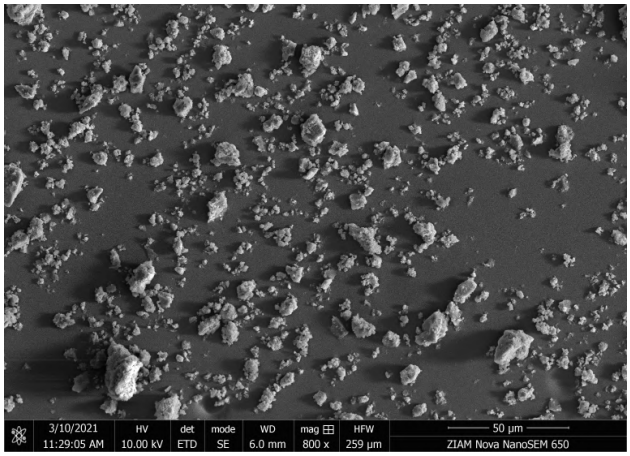

(u) 60_450 Image 4

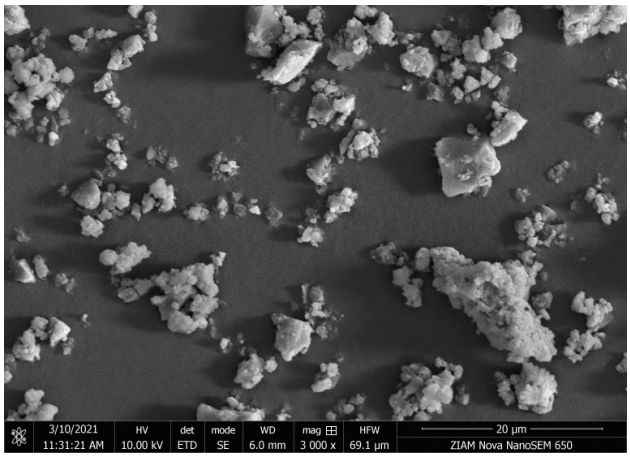

(v) 60_450 Image 5

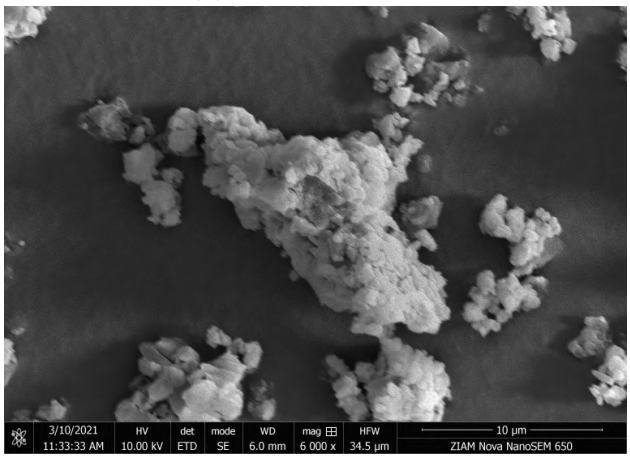

(w) 60_450 Image 6

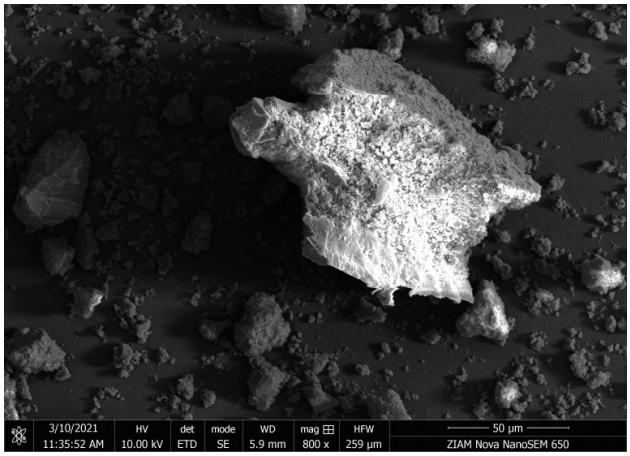

(x) 60_450 Image 7

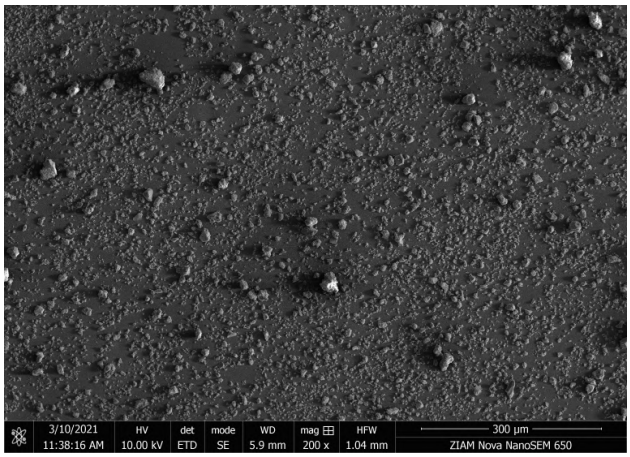

(y) 60_450 Image 8

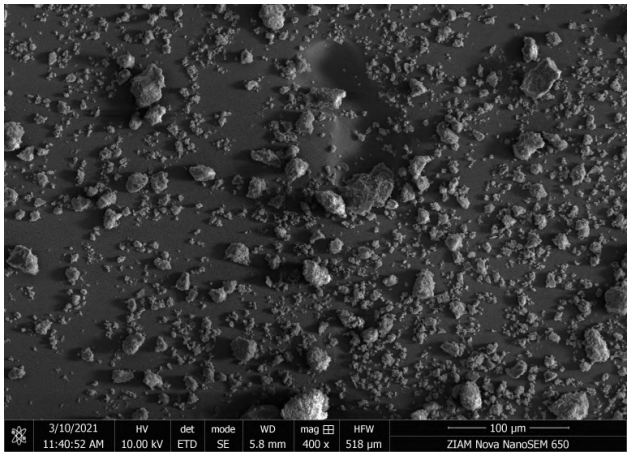

(z) 60_450 Image 9

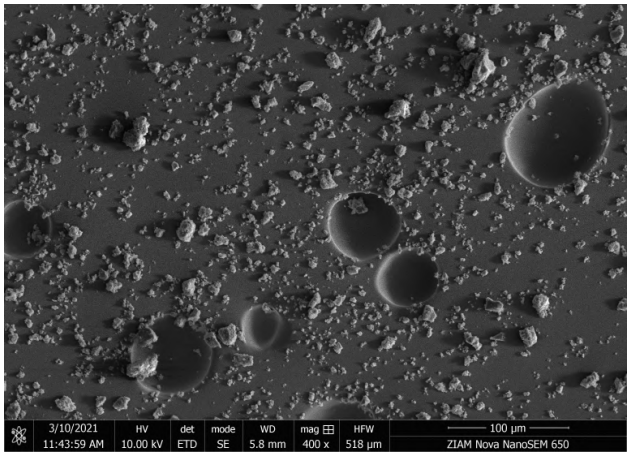

(aa) 60_450 Image 10

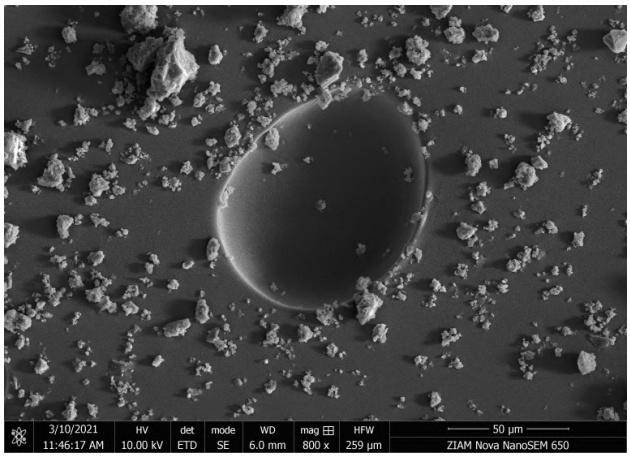

(ab) 60_450 Image 11

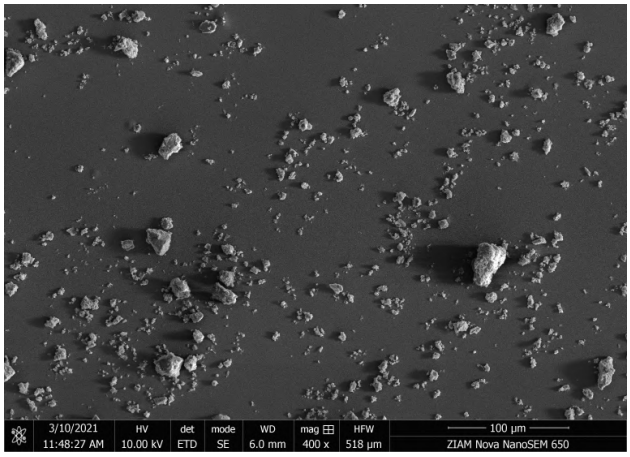

(ac) 60_450 Image 12

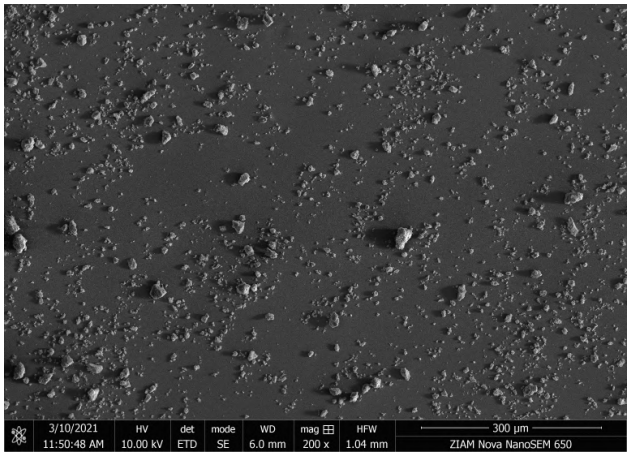

(ad) 60_450 Image 13

A.2 SEM Analysis results

imagefile:	10032021_Kraft lignin_0 min_004.png
scale:	500 µm = 744 px

diameter (px)	diameter (µm)
214	144
122	82
50	34
175	118
22	15
20	13
104	70
134	90
47	32
62	42
33	22
53	36
45	30
90	60
66	44
55	37
84	56
104	70
119	80
52	35
38	26
55	37
131	88
17	11
17	11
50	34
78	52
178	120
183	123
131	88
112	75
40	27
43	29

18	12
83	56
98	66
76	51
108	73
85	57
32	22
75	50
16	11
81	54
43	29
72	48
36	24
75	50
113	76
83	56
80	54
57	38
65	44
185	124
75	50
70	47
14	9
83	56
76	51
74	50
102	69
8	5
52	35
18	12
84	56
27	18
29	19
26	17
18	12
27	18
101	68
74	50
23	15
77	52

115	77
26	17
101	68
51	34
38	26
27	18
38	26
61	41
19	13
45	30
26	17

imagefile:	10032021_Kraft lignin_10 min_007.png
scale:	50 µm = 596 px

diameter (px)	diameter (µm)
608	51.0
54	4.5
78	6.5
114	9.6
158	13.3
117	9.8
57	4.8
47	3.9
68	5.7
187	15.7
179	15.0
57	4.8
77	6.5
106	8.9
133	11.2
174	14.6
137	11.5
107	9.0
99	8.3
126	10.6
189	15.9
77	6.5

88	7.4
65	5.5
75	6.3
61	5.1
117	9.8
176	14.8
64	5.4
71	6.0
61	5.1
96	8.1
72	6.0
69	5.8
42	3.5
89	7.5
209	17.5
113	9.5
96	8.1
72	6.0
56	4.7
63	5.3
85	7.1
106	8.9
44	3.7
100	8.4
57	4.8
35	2.9
81	6.8
98	8.2
56	4.7
52	4.4
56	4.7
49	4.1
49	4.1
42	3.5
60	5.0
42	3.5
39	3.3
48	4.0
44	3.7
35	2.9

41	3.4
57	4.8
35	2.9
46	3.9
41	3.4
44	3.7
43	3.6
68	5.7
36	3.0
42	3.5
64	5.4
38	3.2
44	3.7
51	4.3
49	4.1
65	5.5
44	3.7
45	3.8
36	3.0
51	4.3
40	3.4
33	2.8
35	2.9
21	1.8
31	2.6
21	1.8
28	2.3
24	2.0
24	2.0
30	2.5

imagefile:	10032021_Kraft lignin_60 min_003.png
scale:	50 µm = 596 px

diameter (px)	diameter (µm)
87	7.3
127	10.7
86	7.2

123	10.3
100	8.4
73	6.1
67	5.6
70	5.9
49	4.1
47	3.9
85	7.1
104	8.7
99	8.3
88	7.4
114	9.6
92	7.7
52	4.4
79	6.6
60	5.0
118	9.9
44	3.7
43	3.6
51	4.3
41	3.4
42	3.5
46	3.9
45	3.8
38	3.2
35	2.9
32	2.7
34	2.9
39	3.3
41	3.4
44	3.7
38	3.2
32	2.7
34	2.9
42	3.5
34	2.9
34	2.9
80	6.7
110	9.2
96	8.1

64	5.4
151	12.7
54	4.5
55	4.6
74	6.2
31	2.6
37	3.1
66	5.5
41	3.4
48	4.0
48	4.0
32	2.7
40	3.4
29	2.4
25	2.1
23	1.9
34	2.9
35	2.9
69	5.8
30	2.5
46	3.9
43	3.6
31	2.6
50	4.2
18	1.5
24	2.0
28	2.3
28	2.3
26	2.2
25	2.1
53	4.4
63	5.3
37	3.1
47	3.9
38	3.2
63	5.3
72	6.0
36	3.0
27	2.3
43	3.6

34	2.9
30	2.5
35	2.9
34	2.9
32	2.7
48	4.0
46	3.9
35	2.9
27	2.3
23	1.9
58	4.9
28	2.3
25	2.1
17	1.4
25	2.1
24	2.0
25	2.1
41	3.4
29	2.4
37	3.1
24	2.0
24	2.0
23	1.9
18	1.5
30	2.5
28	2.3
30	2.5
20	1.7
35	2.9
34	2.9
32	2.7
32	2.7
26	2.2
31	2.6
27	2.3
38	3.2
27	2.3
28	2.3
29	2.4
40	3.4

32	2.7
40	3.4

Table A.3: Ball milled particle size measurements

Table A.1: Cumulative Frequency distribution

Range (µm)	Mean of range (µm)	Cumulative Frequency 0_450	10_450	60_450
150-250	200	1.000	1.000	1.000
100-150	125	1.000	1.000	1.000
75-100	87.5	0.940	1.000	1.000
50-75	67.5	0.845	1.000	1.000
30-50	40	0.571	1.000	1.000
20-30	25	0.333	1.000	1.000
10-20	15	0.226	1.000	1.000
7-10	8.5	0.024	0.890	0.976
5-7	6	0.000	0.725	0.880
3-5	4	0.000	0.516	0.776
2-3	2.5	0.000	0.132	0.456
1-2	1.5	0.000	0.022	0.056
0-1	0.5	0.000	0.000	0.000

Appendix B

HDO

B.1 Mass balance and experimental data

Date:	07-05-21		17-05-21		26-05-21	
Label:	08 (unmilled)		09 (36 min)		10 (5 min)	
	Before	After	Before	After	Before	After
Lignin	15.25		14.99		15.56	
Catalyst	0.7634		0.7584		0.7566	
P (bar)	103	45	98	43	100	44
T (degC)	22	22	21	40	22	32
Filter paper	1.89	3.76	1.85	3.44	1.89	3.56
Beaker Acetone	106.86	109.16	101.82	105.3	101.81	105.84
Vial H2O	17.86	19.25	18	18.93	17.88	18.91
LO vial	36.01	41.01	17.92	21.34	17.83	20.71
Reactor + stirrer	1952.81	1965	1952.36	1965.12	1952.38	1965.36

Date:	28-05-21		14-06-21		15-06-21	
Label:	11 (5 min)		14 (10 min)		15 (20 min)	
	Before	After	Before	After	Before	After
Lignin	15.02		14.47		15.04	
Catalyst	0.7506		0.743		0.750	
P (bar)	100	40	100	40	101	41
T (degC)	21	21	23	25	22	24
Filter paper	1.91	3.3	1.92	3.56	1.95	3.45
Beaker Acetone	124.85	129.08	124.83	127.91	119.21	123.14
Vial H2O	18.39	19.52	18.32	19.95	18.45	19.89
LO vial	18.34	22.2	18.43	22.73	18.36	22.32

Reactor + stirrer	1952.4	1964.92	1952.44	1965.48	1952.43	1965.36

Date:	16-06-21		17-06-21		18-06-21	
Label:	16 (20 min)		17 (60 min)		18 (36 min)	
	Before	After	Before	After	Before	After
Lignin	15.35		14.75		15.02	
Catalyst	0.761		0.759		0.775	
P (bar)	101	41	100	43	100	39
T (degC)	26	28	26	32	24	21
Filter paper	1.97	3.38	1.96	3.39	1.88	3.42
Beaker Acetone	103.1	106.44	119.22	122.1	103.13	105.87
Vial H2O	18.3	19.59	18.4	19.85	18.46	19.65
LO vial	18.33	21	18.5	23.34	18.33	23.11
Reactor + stirrer	1952.45	1964.16	1952.44	1966.19	1952.44	1965.62

Date:	22-06-21		25-06-21		28-06-21	
Label:	19 (60 min)		21 (unmilled)		22 (10 min)	
	Before	After	Before	After	Before	After
Lignin	15.22		15.64		14.97	
Catalyst	0.762		0.770		0.760	
P (bar)	100	36	100	39	106	47
T (degC)	25	22	23	25	22	30
Filter paper	1.9	3.7	1.83	3.91	1.89	3.13
Beaker Acetone	103.08	106.5	103.08	105.87	119.22	122.06
Vial H2O	18.39	19.56	18.37	19.76	18.34	19.6
LO vial	18.42	22.38	18.25	21.32	18.45	23.6
Reactor + stirrer	1952.52	1965.4	1952.45	1965.4	1952.61	1965.81

Table B.1: Mass Balance all data

Appendix C

Gas-GC

Table C.1: Gas-GC data: concentrations of low molecular weight gasses (HC C3 and below, H2 and CO and CO2)

Experiment #	0_450 08	36_450 09	5_450 10	5_450 11	10_450 14	20_450 15	20_450 16	60_450 17	36_450 18	60_450 19	0_450 21	10_450 22
CO2	8.56	9.30	9.65	8.47	9.62	9.69	10.02	9.79	9.65	10.10	11.13	8.29
Ethylene	0.00	0.00	0.00	0.00	0.00	0.00	0.00	0.00	0.00	0.00	0.00	0.00
Ethane	2.58	3.03	2.81	2.62	3.27	2.72	3.00	2.71	2.90	3.26	3.30	2.34
Propylene	0.00	0.00	0.00	0.00	0.00	0.00	0.00	0.00	0.00	0.00	0.00	0.00
Propane	1.22	1.34	1.20	1.14	1.45	1.14	1.27	1.26	1.29	1.48	1.45	1.11
H2	52.08	49.30	45.64	45.32	46.71	46.85	45.24	48.17	43.88	45.26	46.14	53.30
CH4	31.95	33.11	33.42	32.06	33.11	34.04	35.58	32.80	34.19	34.19	33.42	28.12
CO	2.44	2.75	1.98	2.31	2.58	1.89	1.86	2.29	2.56	3.57	1.89	2.02

Appendix D

RRF GCxGC

Table D.1: Relative Response Factors (RRF) for identified substances relative to DBE

Compounds	RR Factor
Aromatics	1.234
Cycloalkanes	1.555
Dihydroxybenzenes	0.7
Hydrocarbons	1.501
Ketones	1
Methoxyphenols	0.83
Naphtalenes	1.475
Phenols	1.125